공학석사 학위논문

새로운 질병 진단법 개발을 위한 주사기 필터를 이용한 병원체 핵산 분리 기술 및 정확한 검출 기술 연구

Study for development of a novel disease diagnosis assay using PVDF syringe filter and sensitive detection techniques

울 산 대 학 교 대 학 원

의 과 학 과

이 효 주

새로운 질병 진단법 개발을 위한 주사기 필터를 이용한 병원체 핵산 분리 기술 및 정확한 검출 기술 연구

지 도 교 수 : 김 성 한

이 논문을 공학석사 학위 논문으로 제출함

2022년 08월

울 산 대 학 교 대 학 원

의과학과

이 효 주

이효주의 공학석사 학위논문을 인준함

심사위원 김 성 한 (인)

심사위원 김 준 기 (인)

심사위원 신 용 (인)

울 산 대 학 교 대 학 원

2022년 08월

ABSTRACT

Infectious Diseases caused by bacteria and viruses can lead to major problems, including economic loss and death. Recently, the coronavirus disease (COVID-19) pandemic caused by the severe acute respiratory syndrome coronavirus (SARS-CoV)-2 spread rapidly and severely limited the capabilities of public health communities and systems around the world. Therefore, accurate, rapid, and robust diagnostic tests for infectious diseases are crucial to prevent the further spread of the infection, alleviate the burden on healthcare and diagnostic facilities, and ensure timely therapeutic intervention. Despite the development of various techniques for the rapid and accurate molecular diagnosis of disease, several challenges for diagnosis continue; for example, numerous clinical samples with low concentrations of pathogens, and large instruments, complex manuals, are time-consuming. The problems must be addressed. In this study, we developed a novel disease diagnosis assay using polyvinylidene fluoride (PVDF) syringe filter and sensitive detection techniques that can be used to perform pathogen enrichment, nucleic extraction and accurate detection in clinical specimens.

For the sample preparation step, we developed a commercial hydrophilic PVDF syringe filter to test the collected spiked bacteria and biopsy samples from patients. Because of the pore of membranes and cross-linking reagents like dimethyl pimelimidate (DMP), pathogens were collected at the surfaces of membranes. After the cell lysis step, we extracted nucleic acids. DMP consists of two imidoester groups that react with amine groups of nucleic acids to form amidine bonds and generate electrostatic coupling. This self-powered sample preparation platform can be operated by hand, without the use of any sophisticated instrumentation, and is possible within 30 minutes. Compared to the case extracted with commercial kits, it shows comparable efficiency for the sample preparation.

For the detection step, we developed the detection method of nucleic acids using isothermal amplification with the naked-eye. We used the recombinase polymerase amplification (RPA), Helicase-dependent amplification (HDA) and loop-mediated isothermal amplification (LAMP) as isothermal nucleic acid amplification methods to test SARS-CoV-2 diagnosis. The naked-eye assay with the lateral flow method or colorimetric method was delivered result immediately. The limit of detection using the proposed techniques was higher sensitive than that of the end-point PCR. We validated the accuracy of the system by using 23 clinical nasopharyngeal specimens for COVID-19 detection.

Next, the detection of single point mutation is of great significance in the early diagnosis of cancers, molecular targeted, customized drug delivery guidance, treatment progression, and monitoring of tumor's drug resistance. Existing mutation detection techniques are expensive, complex, allele-specific, or does not allow for multiplex detection at once. Thus, we developed a hot spot-specific probe (HSSP) for the detection of *KRAS* mutation from tissue samples of colorectal cancer (CRC) patients. Without any additional steps, we can detect the mutation with high sensitivity and rapidity by quantitative real-time PCR.

The proposed sample preparation technique in this study provides a simple, reliable, cost-effective, and sensitive platform for use with small to large volumes of clinical samples and thus has tremendous utility for various infectious diseases. In addition, the isothermal amplification methods with the naked eye and HSSP platform offer simple, facile, efficient, and inexpensive diagnosis assays of infectious diseases like COVID-19 and Cancers at home and the clinic as a pre-screening platform to reduce the burden on the medical staff in this pandemic era. Taken together, the integration of the proposed techniques (sample preparation and detection) could be provided a faster and cheaper diagnostic assay than the existing method in clinical applications.

Keywords: Molecular diagnostics, Sample preparation, Point-of-care test, Mutation detection;

CONTENTS

LIST OF TABLES & FIGURES

ABBREVIATIONS

PVDF	Polyvinylidene fluoride
HI	Homobifunctional Imidoester
DMP	Dimethyl Pimelimidate
DW	Distilled Water
$NaHCO_3$	Sodium bicarbonate
NA	Nucleic Acid
SD	standard deviation
FTIR	Fourier-transform infrared
POC	Point-Of-Care
qPCR	Real-time PCR
RT	Reverse Transcription
RT-qPCR	Reverse Transcription real-time PCR
Ct	cycle threshold
RPA	Recombinase-based polymerase amplification
HDA	Helicase-dependent amplification
LAMP	Loop-mediated isothermal amplification
LFA	lateral flow assay
HSSP	Hot spot-specific probe
CRC	Colorectal cancer
KRAS	Kirsten rat sarcoma viral oncogene homologue

1. INTRODUCTION

Currently, infections from highly contagious pathogens are spreading around the world, especially, new mutant infectious agents are being discovered [1]. Pandemics caused by infectious diseases such as COVID-19 have had a significant impact on health care and medical support worldwide due to the increase in suspected cases as well as massive social losses [2-4]. In the case of this severe acute respiratory syndrome coronavirus 2, symptoms vary from individual to individual [5, 6], and isolation and treatment of patients through rapid diagnosis are important to prevent the spread of this disease [7]. As a result of this, healthcare workers have faced the burden of many diagnostic tests, and to solve this problem, a quick, accurate, and simple self-diagnosis method for COVID-19 has become very necessary.

Many methods of separating and detecting different biomarkers used in molecular diagnosis are being studied. In particular, other approaches for NAs extraction have developed rapidly in the past century and have been applied to disease diagnosis [8]. Currently, the main methods of NAs extraction are the concentrated salt method, anion decontamination method, water extraction method, phenol extraction method, and enzyme hydrolysis method [9]. The most widely used techniques are based on density gradient centrifugation and culture [10, 11]. However, this method still has many problems [12]. Examples include expensive extraction kits and equipment, time-consuming due to complex protocols, limited sample volumes, and inaccurate results due to external contamination [13-15]. Since the pathogen concentration is very low in the early stages of the disease, very specific and sensitive methods are needed for effective early diagnosis and monitoring. Above all, the concentration method of pathogens based on sample preparation is very important because it correlates highly with the sensitivity of pathogen detection in clinical applications.

The detection technique of COVID-19 is mainly used for nucleic acid-based molecular diagnosis [16-19]. Quantitative polymerase chain reaction (qPCR) is the most widely and commonly used method [20-22]. This method is sensitive, and specific, but relatively time-consuming, and requires personnel with specific equipment, expensive reagents, and specialized skills. To overcome these limitations, this study used isothermal amplification methods such as recombinase-based polymerase amplification (RPA), helicase-dependent amplification (HDA), and loop-mediated isothermal amplification (LAMP). In particular, virus detection methods using LAMP are rapidly developing [23-25]. The LAMP method is simple and fast, with no additional large equipment and no trained professionals [26, 27]. After the amplification process, we tried to provide a convenient, fast, and inexpensive approach for sensitive and specific detection. To this end, lateral flow analysis (LFA) has been widely used for virus detection [28]. The colorimetric RT-LAMP analysis extends the underlying LAMP technique and includes a one-port response based on visual detection of NA amplification [29]. LFA and colorimetry are portable, and the results are visually observable [29-31]. Therefore, such a method may be used for diagnostic purposes in areas, POC centers, or sites where instrumentation is insufficient.

The colorectal cancer (CRC) is the third-largest incidence and second-largest mortality rate worldwide [32-35]. In this CRC, about 20% of patients are diagnosed as metastatic diseases [36]. This metastatic CRC also was associated with lower disease-specific survival, so had less than 14% of the 5-year survival rate [37]. During metastatic CRC, *KRAS* mutates between 30 and 40%, and 90% of these mutations occur in codons 12 and 13 [38, 39]. The *G12D* type is occurred in codon 12 and has the highest incidence among *KRAS* mutations. The *G13D* type is occurred in codon 12 and was found most frequently in CRC [39]. Several studies have demonstrated that these *KRAS* mutations are being used as prognostic

biomarkers. Most commonly used as a biomarker for anti-EGFR drug treatment, it is widely recognized that the lack of response to drugs such as Cetuximab and Panitumab, anti-EGFR MoAbs, occurs in wild-type *KRAS* mutations. Due to these findings, the European Medicines Agency and the Food and Drug Administration have restricted the use of Cetuximab and Panitumab only in patients with wild-type *KRAS* tumors [40-43]. As such, nucleic acid sequence variables are a key goal of economical and high throughput detection and quantification, and detecting and profiling rare nucleic acid mutations with low allele frequencies such as cancer mutations or resistance is a challenge in current molecular diagnostic techniques. Gene mutation detection technology provides the best customized treatment for each patient and has significant implications for early diagnosis, treatment progression, and tumor drug resistance monitoring [44-46]. The gold standard for detection of mutations is to determine bases such as next-generation sequencing (NGS) and sanger sequencing. However, sequencing techniques are complex, time-consuming, and expensive. In addition, for determination of mutant subgroups through direct sequence, mutant cells must exist at a minimum concentration of up to 30% of the total gene content [47, 48]. The oncoBEAM technique and the Idylla method show a limited sensitivity of 1% to 5% with respect to detection of *KRAS* alleles with few mutations. But you need specific equipment that's expensive [49]. To address these shortcomings, many new methods based on polymerase chain reactions (PCRs) to detect *KRAS* mutations have been studied. There are methods such as PCR restriction fragment length polymorphism mapping (PCR-RFLP), allele-specific PCR (AS-PCR), and droplet digital PCR (ddPCR). It is limited to simultaneous analysis of different types of genome mutations [50]. Furthermore, recent studies show that detection kits from different manufacturers show inconsistent results even if the same billing LOD is used for *KRAS* mutation detection [51]. Conventional methods using quantitative PCR are used to detect the presence and frequency of mutations using

fluorescent probes specific to wild-type and mutant alleles. This method is highly sensitive and reliable, but detects only one mutation encoded in the probe [52]. In addition, sequence selection blockers were used to recognize mutations and increase discrimination efficiency between different types of mutations or wild types. To date, many methods have been studied using sequence selection blockers to distinguish mutations by blocking wild types [44, 47, 53]. Hence, a novel detection technique including single point mutation would be desired at poorly equipped or understaffed health centers, and when results are urgently needed for optimal diagnosis of emerging infectious diseases and human cancers.

For the diagnosis of infectious disease, we present a simple and fast new sample preparation method called the DMP-PVDF platform. As a method of using a homobifunctional imidoster (HI) material and a syringe filter, HI is used as a cross-linker agent that forms an amine by biocovalently bonding through the reaction of two imidoster groups and primary amine groups [54]. Various studies have demonstrated that this is a reagent that binds to pathogens through electrostatic interactions and can capture nucleic acids by recognizing the terminal amino groups of nucleic acids [55-57]. Dimethyl Pimelimate (DMP) is one of the HI materials. The polyvinylidene fluoride (PVDF) syringe filter used with DMP contains a PVDF membrane, and the membrane is hydrophilic. The existing Syringe filter was widely used to remove contaminants. In this study, we will concentrate pathogens and extract nucleic acids using membrane-separated ones. This method proved its potential using bacterial samples. In addition, it shows its availability in clinical practice by concentrating SARS-CoV-2 virus. This new technology, including the DMP-PVDF platform and the RT-LAMP method for naked-eye detection, can make diagnosis easier, more efficient, and cheaper. The combination of RT-LAMP analysis and DMP-PVDF filters for enrichment, amplification, and detection of viral RNA increases sensitivity and specificity, while reducing the risk of

contamination and eliminating the need for sophisticated tools or complex processes. The proposed system detects viral RNA in 2.33×10^2 dilutions per reaction. In addition, we tested 23 nasopharyngeal clinical samples to verify the clinical usefulness of rapid COVID-19 molecular diagnostic systems. Using this system, SARS-CoV-2 extracted from human samples was simultaneously concentrated, amplified, and highly sensitive within 60 min.

Next, for the diagnosis of cancer, we present a study to detect the mutation using real-time PCR with hotspot-specific probe (HSSP) to challenge the limitations of existing methods. With this proposed method, we confirmed that the sensitivity was 88.86%, and the specificity was 94.38% in clinical samples. This method is faster, cheaper, more sensitive, and exhibits significant results for mutation detection in clinical samples.

Although the proposed techniques have been demonstrated separately, the proposed techniques should be integrated for further study. Further validation is also required in more clinical samples to improve versatility and ensure the usefulness of this system in clinical applications. We envision that the integrated system with the proposed sample preparation and detection techniques would be useful for disease diagnosis in clinical applications.

2. MATERIALS AND METHODS

2-1 Sample preparation of the DMP-PVDF platform

The platform uses commercially available products such as syringes and ABLUO Syringe PVDF filters (0.45 μm, 13 mm, GVS, Bologna, Italy). Additionally, Dimethyl Pimelimidate (DMP), which is Homobifunctional Imidoester (HI), was used to increase efficiency. The interaction of NAs and DMP on a PVDF membrane was characterized using Fourier-transform infrared (FTIR) spectroscopy (JASCO 6300, JASCO, Easton, MD, USA)

The procedure for pathogen or virus enrichment was as follow steps: (1) 300 μL of DMP (100 mg/mL) was pipetted into sample. The mixture was inserted into the PVDF syringe filter. (2) The PVDF syringe filter with mixture was incubated for 10 min at room temperature to allow pathogen or virus capture. (3) The PVDF syringe filter was washed with 1 mL PBS to remove debris. (4) The enriched solution was collected using an elution buffer (10 mM sodium bicarbonate, $NaHCO_3$, pH 10.6). (5) The NAs of the enriched solution were extracted using the QIAamp Viral RNA Mini Kit (Qiagen, Hilden, Germany) or QIAamp DNA mini kit (Qiagen) according to the manufacturer's instructions. This DMP-PVDF platform is possible to pathogen enrichment and NAs extract at once. After enrichment step (2), the process for NA extraction was as follow steps: (3) It was added to lysis mixture containing 150 μL lysis buffer (100 mM Tris-HCl (pH 8.0), 10 mM EDTA, 1 % SDS, 10 % Triton X-100), 150 μL DMP (100 mg/mL), and 20 μL Proteinase K (Qiagen) in PVDF syringe filter enriched pathogen. Selectively, for RNA extraction, the lysis mixture was added to 30 μL of DNase (Qiagen). (4) The mixture was inserted into the PVDF syringe filter and incubated for 20 min at 56 °C or room temperature for DNA and RNA extraction, respectively. (5) The washing step was processed with 1 mL PBS. (6) Afterward, the NAs were extracted from the PVDF syringe filter using the elution buffer.

2-2 PCR and sequencing analysis

The end-point PCR conditions were as follows: an initial denaturation step at 95 °C for 15 min; 45 cycles at 95 °C for 30 s, 58 or 63 °C for 30 s, and 72 °C for 30 s; and extension step at 72 °C for 5 min. 5 μL of DNA was amplified in a total volume of 25 μL, containing 10X PCR buffer (Qiagen), 2.5 mM $MgCl_2$, 0.25 mM deoxynucleotide triphosphate, 2.5 μM of each primer, and 1 unit of Taq DNA polymerase (Qiagen). The PCR was performed on a T100TM Thermal Cycler (Bio-Rad, Hercules, CA, USA), and were analyzed by electrophoresis on a 2% agarose gel. The gel was visualized using a ChemiDoc XRS+ System (Bio-Rad). The qPCR cycling conditions were as follows: an initial denaturation step at 95 °C for 15 min; 45 cycles at 95 °C for 10 s, 58 °C for 20 s, and 72 °C for 20 s; and melting steps at 95 ℃ for 30 s, 65 ℃ for 30 s, and 95 ℃ for 30 s. Amplification reactions containing 5 μL of DNA were performed with AccuPower 2X GreenStar qPCR Master Mix (BIONEER, Daejeon, Korea) in a QuantStudio 3 Real-Time PCR (Applied Biosystems, Waltham, MA, USA) in accordance with the manufacturer's instructions. The detailed sequence of primers used in PCR is shown in Table 1. For direct sequencing of NAs, all the NAs samples were amplified and were then purified by using the Expin PCR SV (GeneAll, Seoul, Korea). The purified samples were directly sequenced using ABI's 3730XL system (Applied Biosystems) with the forward primer at the Macrogen sequencing center (Macrogen Inc. Seoul, Korea).

2-3 Reverse Transcription PCR

The amplification conditions for the RT-PCR were as follows: RT at 50 °C for 30 min; an initial denaturation step at 95 °C for 15 min; 45 cycles at 95 °C for 30 s, 58 °C for 30 s, and

72 °C for 45 s; and an extension step at 72 ℃ for 10 min. 5 μL of RNA was amplified in a total volume of 25 μL, containing 2X PHyperscrit™ One-Step RT-PCR Master Mix (GeneAll). The RT-PCR was performed on a T100TM Thermal Cycler (Bio-Rad). The amplification conditions for the RT-qPCR were as follows: RT at 50 °C for 20 min; an initial denaturation step at 95 °C for 15 min; 40 cycles at 95 °C for 10 s, 58 °C for 20 s, and 72 °C for 20 s; and melting steps at 95 ℃ for 30 s, 65 ℃ for 30 s, and 95 ℃ for 30 s. Amplification reactions containing 5 μL of RNA were performed with AriaMx SYBR Green RT-QPCR Master Mix (Agilent Technology). The RT-qPCR conditions for viral RNA like SARS-CoV-2 were as follow cycling: RT at 50 °C for 10 min; an initial denaturation step at 95 °C for 30 s; 40 cycles at 95 °C for 5 s, 60 °C for 30 s; and cooling steps at 40 °C for 30 s. Amplification reactions containing 5 μL of RNA were performed with LightCycler® Multiplex RNA Virus Master (Roche, Germany). The RT-qPCR was performed on a CFX96 Touch Real-Time PCR Detection System (Bio-Rad) in accordance with the manufacturer's instructions.

2-4 Isothermal amplification and Naked-eye detection methods

In this study, a total of three isothermal amplification methods were used Recombinase-based polymerase amplification (RPA), thermophilic Helicase-dependent amplification (HDA), and Loop-mediated isothermal amplification (LAMP). The primers sequences detailed for each isothermal PCR assay are presented in Table 1. For LFA, the 5`-end of F primer or LF primer was labeled with carboxyfluorescein (FAM) and the 5`-end of R primer or LB primer was labeled with biotin.

The RT-RPA was performed using the 3 μL RNA and a TwistAmp® RT Basic kit (TwistDX, Cambridge, UK); the incubation lasted 25 min at 40 ℃. To evaluate the RT-thermophilic HDA assays, we used the IsoAmp® II Universal tHDA Kit (New England

Biolabs, Beverly, MA, USA). The HDA reaction was performed using a mixture of 5 μL RNA, primers, 25 μL reaction buffer (10X PCR Buffer, MgSO4 (100 mM), NaCl (500 mM), dNTP, IsoAmp enzyme), and ProtoScript ll RT enzyme (PROMEGA, Madison, Wisconsin, USA); It was performed at 42 °C for 2 min, 65 °C for 90 min on a T100TM Thermal Cycler (Bio-Rad). The RT-LAMP was performed using a WarmStart LAMP 2X Master Mix (NEB) and used with primer solution containing all LAMP primers (1.6 μM for FIP/BIP, 0.2 μM for F3/B3, and 0.4 μM for LF/LB.) and 5 μL RNA. The RT-LAMP reactions were incubated at 65 °C for 30 or 60 min on a T100TM Thermal Cycler (Bio-Rad). For colorimetric RT-LAMP detection, the WarmStart Colorimetric LAMP 2X Master Mix (NEB) was mixed with primer solution containing all LAMP primers and 5 μL RNA templates. The reactions were performed at 65 °C for 30 or 60 min, and a color change from red to yellow was observed for the positive sample.

The amplified products were analyzed on a 2 % agarose gel and with an LFA using the Milenia HybriDetect 1 kit (TwistDx). A 5 μL sample of amplification was mixed with 100 μL of an LFA dilution solution (TwistDx) at a new tube, and then placed on a sample pad of a lateral flow strip (TwistDx). Lateral flow strips were immersed in the mixed solution, and the amplified products were observed to make lines. The line was evaluated as either positive like the bottom line of the strip or negative like the control line, the top line of the strip after 1~2 min.

2-5 Mutant detection using HSSP

For mutation detection, the method using Hot Spot-Specific Probe (HSSP) was studied to prevent mutation amplification. The primer and HSSP sequences are listed in Table 1. Primer has 133bp of amplification product size suitable for use in qPCR and contains a point mutation. Among them, reverse primers are designed to be close to point mutations. The

HSSP was overlapped eight nucleotides with the 3' end of the reverse primer and includes mutations, so it is designed to attach only to the targeted mutation. Additionally, it was modified with a C3 spacer at the 3'-end because should not be amplified. Adding this modification to the 3′-end can prevent elongation during PCR without significantly affecting the annealing properties [58, 59]. Thus, this attached HSSP prevents to the targeted DNA amplification.

The qPCR with HSSP cycling conditions were as follows: an initial denaturation step at 95 °C for 15 min; 45 cycles at 95 °C for 10 s, 63 °C for 20 s, and 72 °C for 20 s; and melting steps at 95 ℃ for 30 s, 65 ℃ for 30 s, and 95 ℃ for 30 s. Amplification reactions containing 5 μL of DNA were performed total 25 μL with AccuPower 2X GreenStar qPCR Master Mix (BIONEER) and 2.5 μM primer and 25 μM HSSP in a QuantStudio 3 Real-Time PCR (Applied Biosystems) in accordance with the manufacturer's instructions. The concentration of HSSP was determined for an optimization experiment. The concentration is ten times that of a primer.

2-6 Biological samples

To experiment with the DMP-PVDF platform, we used the extracted DNA from *Escherichia coli (E. coli)* bacteria cells and the extracted RNA from *Brucella ovis (B. ovis)* bacteria cells. *E. coli* (ATCC 25922) was inoculated in nutrient broth medium and incubated overnight at 37 °C under shaking conditions. *B. ovis* (ATCC 25840) was grown in Brucella agar containing 5% defibrinated sheep blood and incubated at 37 °C in a 5% CO2 atmosphere for 48 h. In addition, to identify the DMP-PVDF platform's capacity for quantitation of SARS-CoV-2 viral load, viral RNA was extracted from the culture fluid of SARS-CoV-2-infected VeroE6 cells (Zeptometrix, Cat. No. 0810590CFHI).

Mutation detection using HSSP experimented with *G12D* mutation and *G13D* mutation of *KRAS* mutations. The G12D point mutation was confirmed with the AGS cell line (ATCC_CRL-1739) from isolated the stomach tissue with gastric adenocarcinoma, and the G13D point mutation was confirmed with the HCT116 cell line (ATCC_CCL-247) from the isolated colony of the colon cancer patient. The cells were cultured in high-glucose Dulbecco's modified Eagle's medium (DMEM, HyClone, Logan, UT, USA) supplemented with 10% fetal bovine serum (FBS, HyClone) and 1% antibiotic-antimycotic (Gibco, Grand Island, NY, USA). The cell culture was maintained in plastic culture dishes and incubated in a humidified atmosphere of 5% CO_2 at 37 °C. Subcultures were made at a ratio of 1:3 when the cell density reached 80–90% every 3 or 4 days

To evaluate the limit of detection of the RT-isothermal amplification assays, transcribed T7 RNA was generated with SARS-CoV-2. To prepare the RNA standard, the spike (S) and nucleocapsid (N) genes (GenBank MN908947.3) of SARS-CoV-2 were amplified from a positive clinical sample with primers containing the T7 promoter sequence. The T7-flagged PCR product was synthesized for transcription using a MEGAscript kit (Ambion, Invitrogen, USA). Then, RNA was purified with a MEGAclear kit (Ambion) following the manufacturer's instructions.

To confirm the limit of detection (LOD) and efficiency for HSSP, Mutation DNA templates were made using DNA extracted from the AGS and HCT116 cell lines. The DNA was extracted using the QIAamp DNA mini kit (Qiagen). In addition, in the case of the wild type, a template was made with DNA obtained from a sample of a patient diagnosed with the wild type. The DNA template has a length of 777 bp containing KRAS mutation. DNA templates are made by performing PCR using a designed primer and were then purified by using the Expin PCR SV (GeneAll). Thus, produced DNA template concentration and quality was assessed using a Qubit 3 Fluorometer (Thermo Fisher Scientific, Waltham, MA, USA) and

the DNA copy number was calculated using the EndMemo DNA/RNA copy number calculator (http://endmemo.com/bio/dnacopynum.php). The DNA template was stored at –20°C until use.

2-7 Clinical samples

The clinical samples used in this study are nasopharyngeal samples and tissue samples. For DMP-PVDF platform with isothermal PCR method, the nasopharyngeal specimens were collected from patients infected with human SARS-CoV-2, human coronavirus (HCoV)-OC43/229E, and healthy controls who agreed to sampling and were admitted to Asan Medical Center (AMC), Republic of Korea. This study was reviewed and approved by the ethics committee of the institutional review board of Asan Medical Center, and all participants gave written informed consent. All experimental procedures were performed following the guidelines approved by the Institutional Review Board of AMC (IRB No. 2020-0297). The nasopharyngeal swabs were stored in a universal transport medium (Noble Biosciences, Korea). Clinical specimens were inactivated by heating at 60 °C for 30 min and then stored at −80 °C until using. And, A total of 69 cancer samples (25 samples with G12D mutations, 25 samples with G13D mutation, and 19 samples with no mutation in exon 2) based on frozen tissue availability were obtained from the BRC of AMC, after approval from the Institutional Review Board (IRB_Nr. 2016–0809). Pre-collected databases of clinical pathological characteristics of all patients known to be related to the CRC process are described in previous studies [60]. The genomic DNAs from the tissues were extracted using ATL buffer with proteinase K from a QIAamp DNA mini kit (Qiagen) according to the manufacturer's instructions. The samples were eluted using 100 μL of elution buffer. The eluted DNA was stored at –20 °C until use.

Table 1 Primer sequences

Primer	Sequences 5′-3′	Primer	Sequences 5′-3′
E.coli-F	CAACGAACTGAACTGGCAGA	*B. ovis*-F	GCTTGAAGCTTGCGGACAGT
E.coli-R	CATTACGCTGCGAGGAT	*B. ovis*-R	GGCCTACCGCTGCGAAT
KRAS 777bp-F	TAGCCGCCGCAGAACAGCAGTC	KRAS qPCR-F	GCTGTATCGTCAAGGCACTCTT
KRAS 777bp-R	TCACAATACCAAGAAACCCATAAA	KRAS qPCR-R	ACCTTATGTGTGACATGTTCTAATATAGTC
KRAS G13D HSSP	GCACTCTTGCCTACGTCACCAGCAAAT - 3′C3 spacer	KRAS G12D HSSP	GCACTCTTGCCTACGCCATCAGCAAAT - 3′C3 spacer
S gene T7-Fragment-F	AGAACTCAATTACCCCCTGCAT	N gene T7-Fragment-F	TTTGGTGGACCCTCAGATTC
S gene T7-Fragment-R	CGAAAAACCCTGAGGGAGAT	N gene T7-Fragment-R	TTGGCAATGTTGTTCCTTGA
S gene RT-qPCR-F	TCCGCATCATTTTCCACTTTTAA	N gene RT-qPCR-F	TGGCAGTAACCAGAATGGAGAAC
S gene RT-qPCR-R	AAGTCAGACAAATCGCTCCAGGGCAAA	N gene RT-qPCR-R	AGTGAGAGCGGTGAACCAAGA
S gene RT-qPCR-P	TAACGCAGCCTGTAAAATCATCTG	N gene RT-qPCR-P	CGCGATCAAAACAACGTCGGCC
N gene RPA-F	AATAAGCATATTGACGCATACAAAACATTC	N gene HDA-F	TCACTCAACATGGCAAGGAAGACCTTA
N gene RPA-R	AGGCCTGAGTTGAGTCAGCACTGCTCATGGATTGT	N gene HDA-R	CGAATTCGTCTGGTAGCTCTTCGGTAG
S gene LAMP-F3	TCTTTCACACGTGGTGTT	N gene LAMP-F3	TGGCTACTACCGAAGAGCT
S gene LAMP-B3	GTACCAAAAATCCAGCCTC	N gene LAMP-B3	TGCAGCATTGTTAGCAGGAT
S gene LAMP-FIP	CATGGAACCAAGTAACATTGGAAAATTTTCCTGACAAAGTTTTCAGATCC	N gene LAMP-FIP	TCTGGCCCAGTTCCTAGGTAGTTTTTGACGAATTCGTGGTGGTGA
S gene LAMP-BIP	CTCTGGGACCAATGGTACTAAGAGTTTTGACTTCTCAGTGGAAGCA	N gene LAMP-BIP	AGACGGCATCATATGGGTTGCATTTTGCGGGTGCCAATGTGATC
S gene LAMP-LF	GAAAGGTAAGAACAAGTCCTGAGT	N gene LAMP-LF	ACCATCTTGGACTGAGATCTTTCA
S gene LAMP-LB	CCCTGTCCTACCATTTAATGATGG	N gene LAMP-LB	GAGGGAGCCTTGAATACACCA

3. RESULTS

3.1 – Sample preparation using DMP-PVDF platform

3.1.1. Principle and operation of the DMP-PVDF platform

The platform uses commercially available products such as syringes and ABLUO Syringe PVDF filters (0.45 μm, 13 mm). Conventional syringe filters are used to remove foreign substances. However, in this study, the DMP-PVDF platform was applied to pathogen separation and nucleic acid detection by applying separation by a membrane as opposed to conventional ones. The principles of the DMP-PVDF platform are shown in Figure 1.1. To explain the process, step 1 is enrichment of pathogens. The sample was mixed with DMP and transferred to a PVDF syringe filter. The mixture was incubated at room temperature for 10 minutes to allow the pathogen to bind through a covalent bond of DMP and electrostatic bond between the PVDF filter surface and the pathogen. In step 2, it is isolation nucleic acid from the pathogen attached to the membrane. Insert the lysis solution in the Syringe filter without any solution. Later, for the separation of nucleic acids from the cell, incubated 20 min at 56 °C for DNA or at room temperature for RNA. In between, the nucleic acid separated from the cell binds to the DMP and attaches to the membrane. After the isolation step, wash with PBS once to remove any foreign substances and remove the lysis solution that is inhibiting PCR. Finally, step 3 is the nucleic acid elution step. It is eluted using 10 mM sodium bicarbonate with high pH to break the bond between DNA and DMP. The bond of DMP and DNA is a method identified in previous studies [55, 56]. If the pH is too high affect the PCR. So, we used a solution with pH 10.6 that does not affect the PCR. The DMP-PVDF platform can be used in the new sample preparation process and has potential for application. Above all, it is simple, cheap and can only be carried out by hand without other equipment. Also, only the necessary steps can be used. It can be used only enrichment step, since there is no

capacity limitation, more enrichment can be performed. Conversely, only extraction can be performed with a small amount of sample. These results show that pathogen enrichment and nucleic acid extraction can be simply and quickly within 30 minutes without a separate instrument in point-of-care test.

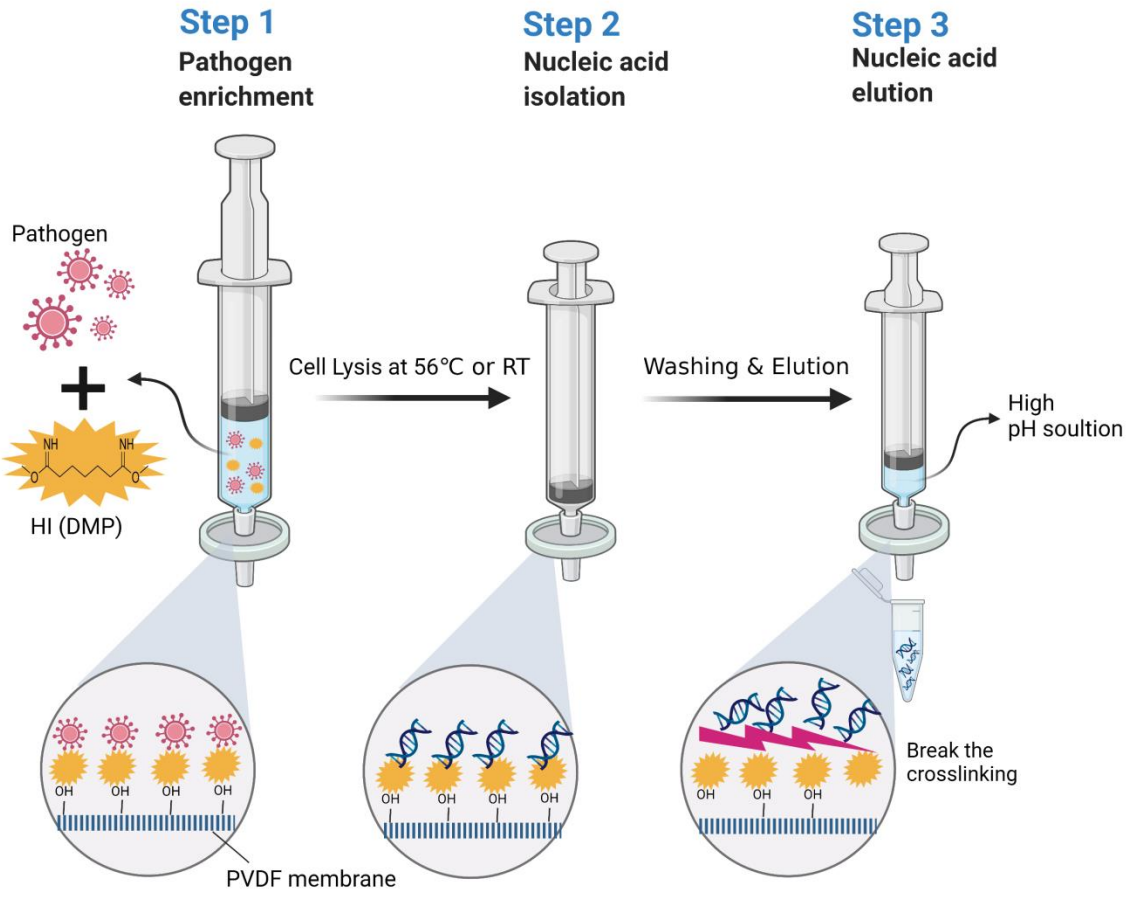

Figure 1.1 Schematic of the principle of Sample preparation using PVDF syringe filter.

(Step 1) Pathogen enrichment step. The capture of the pathogen by DMP via electrostatic interactions. The amine group of DMP enables the pathogen to be enriched on the PVDF membrane surface. (Step 2) Nucleic acid isolation step. Nucleic acid is extracted from the enriched pathogen. Isolation of nucleic acids is performed by injecting a lysis buffer, and incubation is performed at 56℃ for DNA and at room temperature for RNA. The nucleic acids isolated from the pathogen are attached to the amine group of the DMP with an electrical bond. (Step 3) Nucleic acid elution step. Nucleic acid and DMP bond break the bond using an elution buffer with a high pH solution (pH 10.6).

3.1.2. Characterization and application of the DMP-PVDF platform

We confirmed the interaction of NAs and DMP on a PVDF membrane using FTIR spectroscopy. The FTIR spectra results are shown in Figure 1.2. Through Figure 1.2 A, the interaction could be inferred for the results that vary step of pure the PVDF membrane (blue line), and the NAs (pink line), DMP (red line), and combination of the NAs and DMP (brown line) on the PVDF membrane. A distinct absorption peak at 3392 cm^{-1} exhibited the NAs and DMP combination on the PVDF membrane, which is attributed to the O-H/N-H stretching vibrations [61]. The NAs and DMP combination on the PVDF membrane showed higher intensity than each for the characteristic absorption of the wavenumbers; CH_2 asymmetrical stretching variation at 3021 cm^{-1} and 1170 cm^{-1}, and CH_2 symmetrical stretching variation at 2979 cm^{-1} [62-64]. In additional, for the NAs and DMP combination on the PVDF, we established that the characteristic absorptions CH_2 wagging, CF_2 stretching, C-C-C asymmetrical stretching and C-F stretching variations occurred respectively at 1402, 1070, 878, and 834 cm^{-1} [61, 63-66].

Furthermore, the characteristic absorptions for the γ phase occurred at 431, 482, and 1233 cm^{-1}, and the characteristic absorption for the β and γ phases occurred at 510 cm^{-1} for the NAs and DMP combination on the PVDF [67]. These results confirm that the combined DMP and PVDF membrane is higher transmittance than that of the PVDF membrane because of the relative absorption of DMP. Moreover, the FTIR spectra of the NAs and DMP combined on the PVDF membrane were higher transmittance than that of the PVDF membrane because of the relative absorption of the DMP blends and NAs. In Figure 1.2 B, only the membrane was compared to confirm the difference between hydrophilic (black) and hydrophobic (red). For hydrophilic membrane, the peak is shown at 1731 cm^{-1}, unlike hydrophobic membrane. This peak is known to contain carboxylic acid carbonyl [68]. Therefore, it seems that carboxylic acid carbonyl has an effect on the binding of DMP and PVDF membranes.

To test the availability of the sample preparation of the DMP-PVDF platform for the pathogen enrichment and NAs extraction, we used *E. coli* and *B. ovis* as bacteria samples for testing pathogen enrichment and extraction steps. We proved the efficiency of the DMP-PVDF platform for pathogen enrichment and DNA extraction using *E. coli* (10^5 CFU/mL). The positive control was DNA extracted from the absolute concentration *E. coli* (10^5 CFU) sample using a spin column kit. The qPCR *Ct* values of the samples enrichment using the DMP-PVDF platform were lower than those obtained using the PVDF syringe filter without DMP (Figure 1.3 A). This result indicates that the DMP increased the efficiency directly as a cross-linker between the target and the PVDF membrane. Subsequently, we tested the capture efficiency for the pore size and diameter of the filter membrane. Repeat experiments were performed using the filter with different membrane pore sizes and diameters (0.2 μm – 13 mm, 0.45 μm – 13 mm, and 0.45 μm – 25 mm). We observed the highest amplification efficiency with the filter with a 0.45 μm pore size and 13 mm diameter (Figure 1.3 B). Thus, the 0.45 μm – 13 mm membrane was selected and the additional experiment was processed. Furthermore, we determined the capture efficiency of various filter membrane materials. The same experiment was conducted using PVDF, Cellulose Acetate (CA), Polyethersulfone (PES), Nylon (NY), Regenerated Cellulose (RC), Polyethylene (PE), Nitrocellulose (NC), Polytetrafluoroethylene-Hydrophilic (PTFE-HP), or PTEE (Figure 1.3 C). The qPCR *Ct* values of the PVDF membrane was similar to that obtained using the spin column kit. This result showed that the PVDF membrane provided the highest extraction efficiency among the filter membrane materials tested. Unlike the PTFE-HP filter, the PTFE filter was not showed *Ct* values, so it is assumed that extraction is not possible. This shows the difference between the hydrophilic membrane and the hydrophobic membrane. Therefore, these results demonstrate that the PVDF membrane composed of a hydrophilic efficiently capture bacteria and NAs. Next, the efficiency of the DMP-PVDF platform for NAs extraction is dependent

on the elution buffer (Figure 1.3 D). The method was tested using elution buffer of different reagents and pH, such as D.W., AVE buffer (Qiagen kit), 10 mM $NaHCO_3$ (pH 10.6), and 10 mM Tris-HCl (pH 8.0). In the case of Tris-HCl, it is shown that PCR is inhibited and thus not amplified. The highest qPCR *Ct* values of the elution buffer on the DMP-PVDF platform was seen in the 10 mM $NaHCO_3$ with high pH.

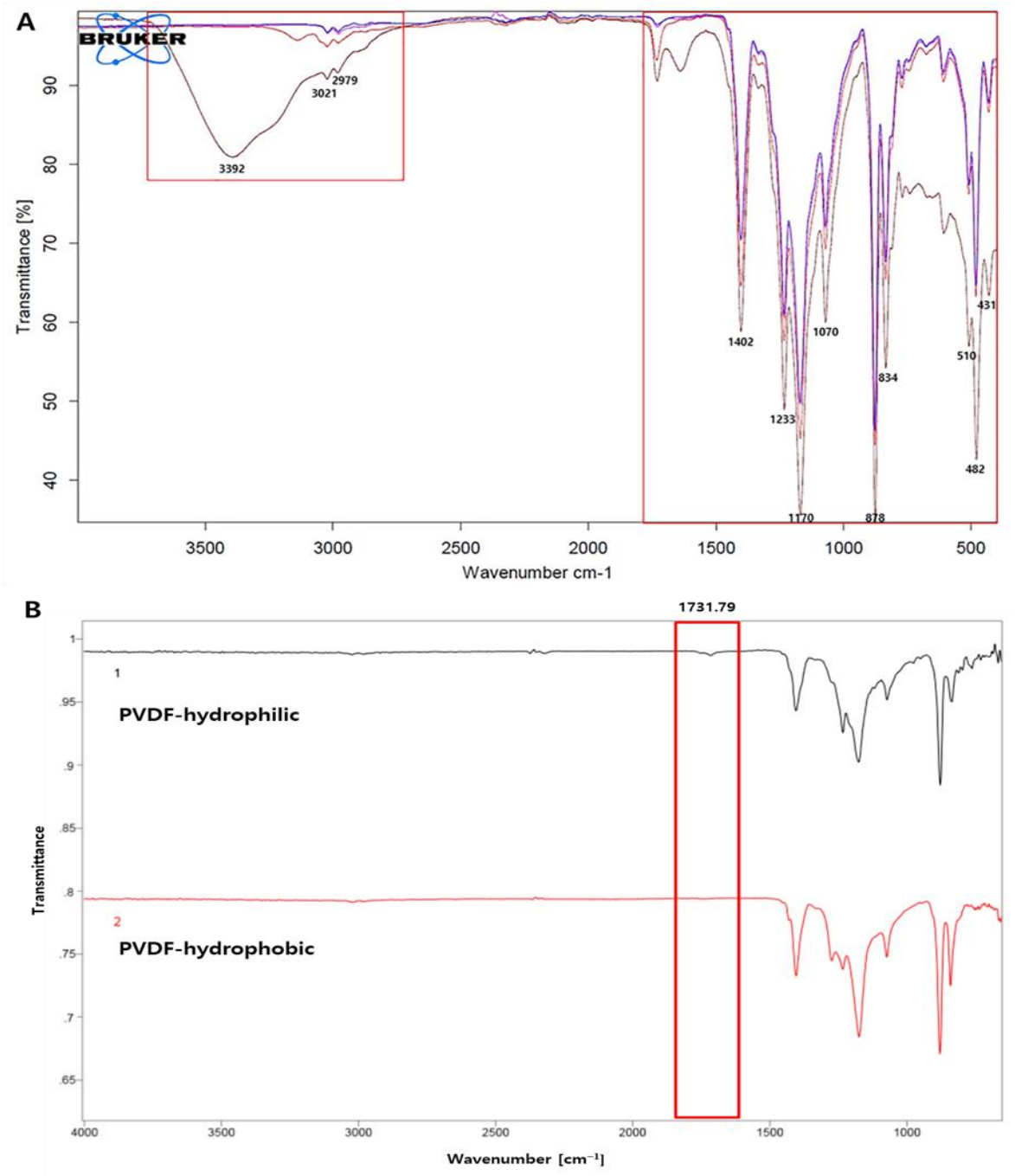

Figure 1.2 Fourier-transform infrared spectra analysis.

(A). The FTIR spectra of the plain PVDF membrane (blue line), NAs (pink line), DMP (red line), and combination of the NAs and DMP (brown line) on the PVDF membrane are indicated. (B). The FTIR spectra of the PVDF-hydrophilic membrane (up), PVDF-hydrophobic membrane (down)

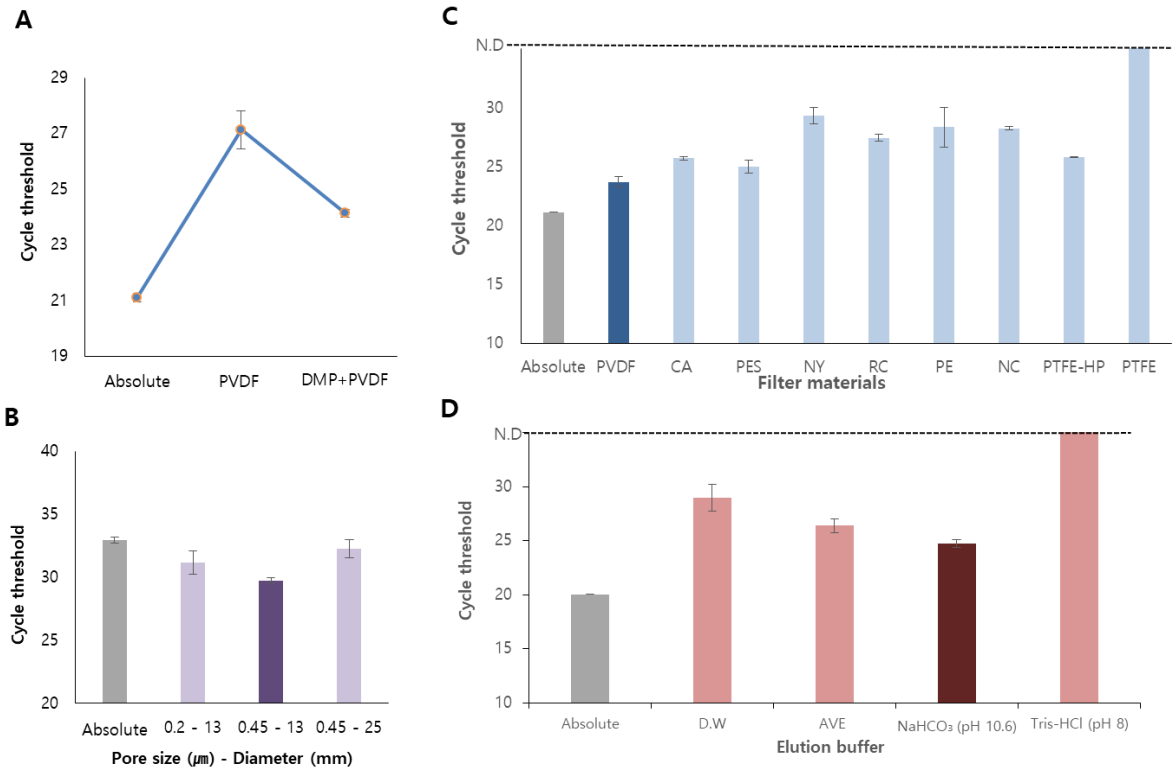

Figure 1.3 Optimization of DMP-PVDF filter platform to pathogen enrichment and extraction.

(A) The efficiency for a sample of *E. coli* (10^5 CFU/mL) following pathogen enrichment and extraction using the DMP-PVDF platform is dependent on DMP. (B) The *E. coli* capture rate of the DMP-PVDF platform depends on the filter membrane pore size and diameter. The nearest and safest value to control (0.45 μm – 13 mm) is marked in purple. (C) The *E. coli* capture rate of the new platform depends on the type of the filter membrane. The PVDF membrane (dark blue) shows the nearest and safest value to control. (D) The efficiency of DMP-PVDF filter platform for pathogen extraction is dependent on the elution buffer. The highest amplification efficiency of the elution buffer was seen the 10 mM $NaHCO_3$ (pH 10.6, dark red). All of the above tests are the same, the absolute control is DNA extracted from 10^5 CFU of *E. coli* by using a Qiagen kit (gray). The data are presented as mean ± SD, based on at least three independent experiments.

3.1.3. Capacity of the DMP-PVDF platform

After optimizing the DMP-PVDF platform for pathogen enrichment and extraction, we evaluated the capacity for sample preparation. The experiment used the *E.coli* for DNA and the *B. ovis* for RNA, and ranging from 1×10^2 to 1×10^5 CFU/mL (Figure 1.4 A and 1.4 B). The qPCR C_t value of the NAs extracted using the DMP-PVDF platform (light green) was lower than those obtained using the spin column kit (gray), which extracted NAs without pathogen enrichment. Moreover, the qPCR C_t value of the DMP-PVDF platform was similar to the absolute value of the pathogen (Qiagen kit, black). These results suggest that the capacity of the DMP-PVDF platform with pathogen enrichment and NAs extraction at once is more efficient than those of conventional commercial kits without pathogen enrichment. Next, we evaluated the capacity of the DMP-PVDF platform with virus enrichment by using SARS-CoV-2 culture fluid ranging from 1×10^1 to 1×10^5 PFU/100μL. SARS-CoV-2 viral loads were analyzed using RT-qPCR assay for targeting the N and S genes (Figure 1.4 C and 1.4 D). The detection limit of the platform is 10 PFU/100μL for both N and S genes. These results suggest that the DMP-PVDF platform can not only be used with NAs extraction but also be used with bacteria or virus enrichment.

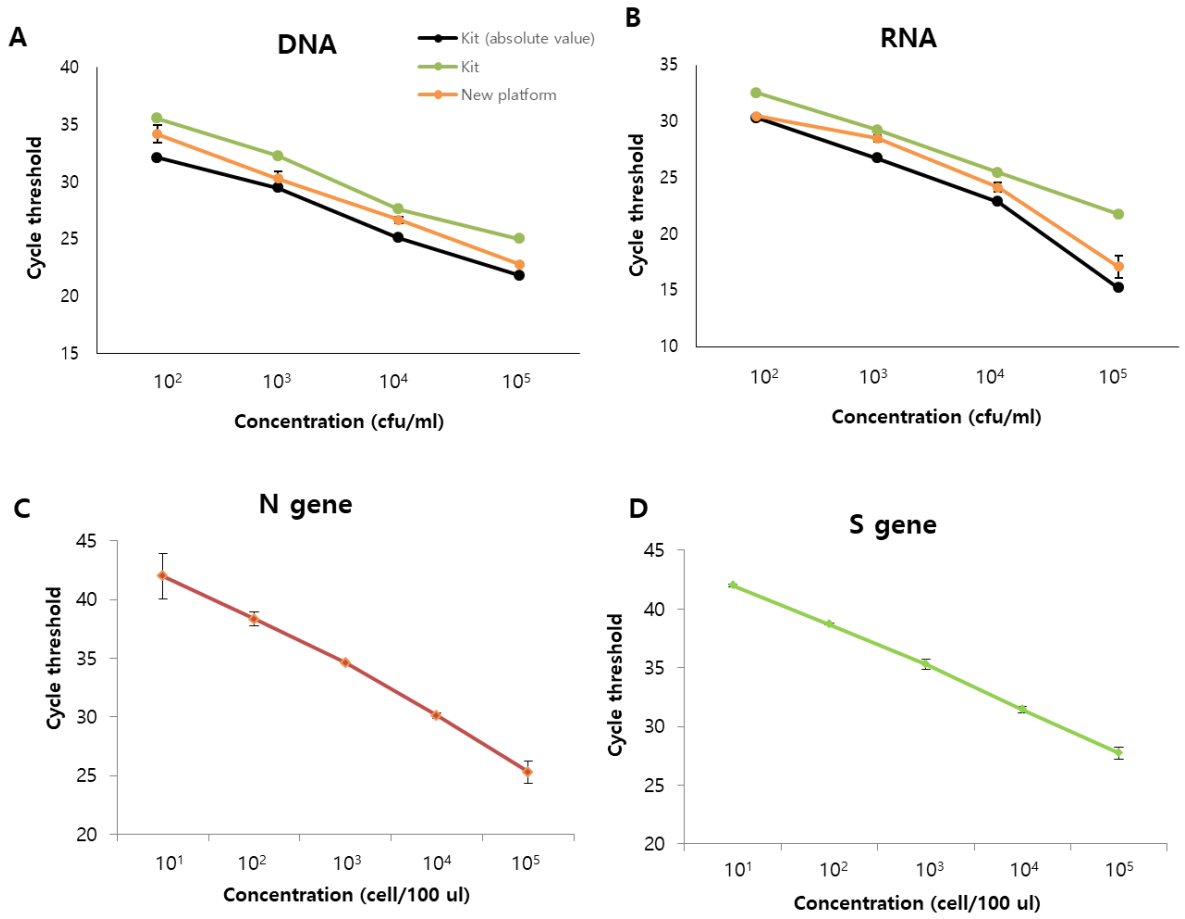

Figure 1.4 Capacity of the DMP-PVDF platform.

(A and B) Concentration for (A) DNA or (B) RNA extraction to process test in concentrations ranging from 1×10^2 to 1×10^5 CFU/mL using both the NA extraction only without enrichment using a Qiagen kit (light green) and the new platform (orange). Black color denotes NA extracted from the absolute concentration sample of using a Qiagen kit. (C and D) Capacity of the DMP-PVDF filter platform to process test SARS-CoV-2 culture fluid ranging from 1×10^1 to 1×10^5 PFU/100μL using a Qiagen kit. SARS-CoV-2 viral loads were quantified using RT-qPCR assay targeting the (C) N and (D) S genes. The data are presented as mean ± SD, based on at least three independent experiments.

3.2 – Detection of SARS-CoV-2 using Isothermal amplification

3.2.1. Principles of procedure for SARS-CoV-2 enrichment and detection

The principles of the rapid COVID-19 molecular diagnostic system for the sample preparation and detection of SARS-CoV-2 are illustrated in Figure 2.1. This system consists of the RT-LAMP and the DMP-PVDF platform. The virus enrichment is processed by the use of the DMP-PVDF platform. Step 1 is the sample preparation stage. For the virus enrichment, we used the DMP-PVDF platform. The samples were mixed with the DMP and inserted into the PVDF syringe filter. The PVDF syringe filter with the sample was incubated for 10 min at room temperature and then washed with 1mL PBS to remove debris. Using an elution buffer, isolate the virus from the PVDF filter and collect it. Subsequently, RNA from the collected virus was extracted using the spin column kit. Step 2 is the RNA detection stage. The RNA extracted was amplified using RT-LAMP. It is one of the isothermal PCR methods, so was faster than conventional PCR. The naked-eye detection used LFA or colorimetric assays. LFA was determined by the number of lines that occurred in the strip. In the case of positive, two lines occurred the test line and the control line. Conversely, in the case of negative, only the control line occurred. Colorimetric assays were determined by a color change from pink to yellow. It contains a pH-sensitive Phenol-red reagent using hydrogen ions that occurred during the amplification process of nucleic acid through RT-LAMP, which changes color. So, after the amplification, yellow was determined to be positive. Therefore, we confirmed that RNA was successfully extracted and detected in both procedures by downstream analysis. This COVID-19 molecular diagnostics system was showed that not only allows for virus enrichment but also for the simple and rapid detection within 60 min.

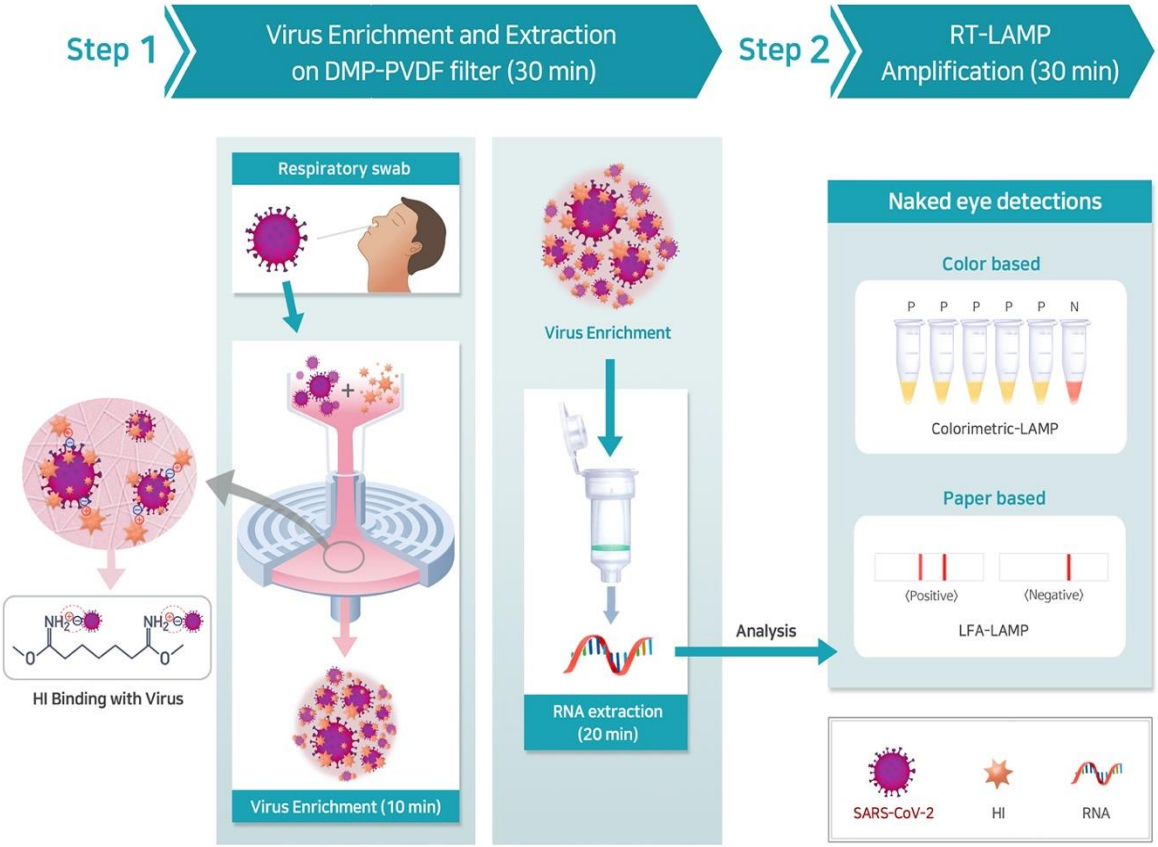

Figure 2.1 The principle of rapid COVID-19 diagnostic system through combining RT-LAMP and DMP-PVDF platform.

(Step 1) Schematic diagram of pathogen enrichment by DMP-PVDF platform. The capture of the virus to the DMP- PVDF platform via electrostatic interactions (left). After incubation for 10 min at room temperature, the virus is collected using an elution buffer. NA is extracted from the enriched virus using a spin column kit (right). (Step 2) The extracted NA is visually confirmed by the naked-eye to RNA detection via colorimetric RT-LAMP (top path) and RT-LAMP with LFA (bottom path).

3.2.2. Isothermal Amplification Assays for SARS-CoV-2 Detection

To determine the RNA detection method for COVID-19 testing, we confirmed the sensitivity of various isothermal amplification methods such as RT-RPA, RT-HDA, and RT-LAMP. The test performed using the template for a ten-fold serial dilution of T7 RNA from the N gene of SARS-CoV-2. The RT-RPA, RT-thermophilic HDA and RT-LAMP were analyzed via either with the LFA or the colorimetric assay for naked-eye detections, and on a 2% agarose gel. The RT-RPA method was performed using T7 RNA copies ranging from 8.12×10^7 to 8.12×10^1 per reaction. The RT-RPA method limit of detection was T7 RNA 8.12×10^3 copies per reaction within 25 min and at a temperature of 40 °C (Figure 2.2 A and 2.2 B). The RT-thermophilic HDA method was performed using T7 RNA copies ranging from 2.59×10^9 to 2.59×10^2 per reaction. The RT- thermophilic HDA method limit of detection was T7 RNA 2.59×10^4 copies per reaction within 90 min and at a temperature of 65 °C (Figure 2.2 C and 2.2 D). Next, the RT-LAMP method was performed using T7 RNA copies ranging from 2.33×10^{10} to 2.33 per reaction. The RT-LAMP method limit of detection was T7 RNA 2.33×10^2 copies per reaction within 60 min and at a temperature of 65 °C (Figure 2.2 E – 2.2 G). These results verify that the LAMP assay provided a relatively sensitive efficiency among these three isothermal amplification assays. Thus, based on the results, the LAMP with either LFA or colorimetric assay for SARS-CoV-2 naked-eye detection was confirmed as the optimal method.

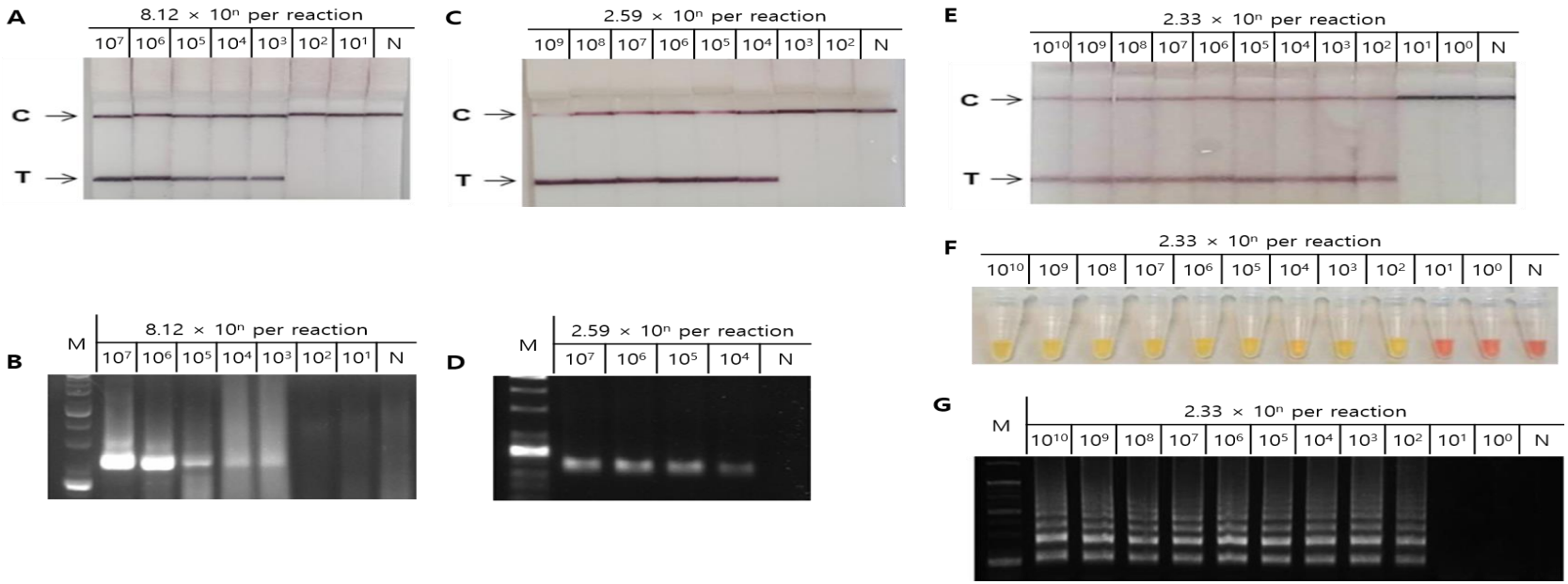

Figure 2.2 Sensitivities of RT-RPA, RT-HDA, RT-LAMP for SARS-CoV-2 detection.

A serial dilution of T7 RNA from the SARS-CoV-2 N gene was used to test the sensitivity of the assay. (A and B) The sensitivity of the RT-RPA method. The reaction products could be detected the T7 RNA (8.12×10^7 to 8.12×10^3 per reaction) on a (A) LFA and (B) 2% agarose gel. (C and D) The sensitivity of the RT- thermophilic HDA method. The reaction products could be detected the T7 RNA (2.59×10^9 to 2.59×10^4 per reaction) on a (C) LFA and (D) 2% agarose gel. (E-G) The sensitivity of the RT-LAMP assay. The reaction products visualized the T7 RNA (2.33×10^{10} to 2.33×10^2 per reaction) on a (E) LFA, (F) 2% agarose gel, and (G) colorimetric RT-LAMP. The limit of detection was 2.33×10^2 of T7 RNA. M, size marker; N, negative control; T, target; C, control.

3.2.3. Optimization of the RT-LAMP Assay for SARS-CoV-2 Naked-Eye Detection

To optimize the LAMP-based assays, which showed the best efficiency among isothermal PCR methods, for SARS-CoV-2 naked-eye detection, LAMP primers were designed to target SARS-CoV-2 with S and N genes. Primer FIP and BIP were modified to include a "TTTT" linker between the F1c and F2 regions as well as between the B1c and B2 regions to further improve the reaction. The designed LAMP primers were confirmed through the RT-LAMP with LFA and colorimetric-LAMP assays. We observed that targeting the S gene detected T7 RNA (5.85×10^9 to 5.85×10^6 per reaction) through the RT-LAMP with LFA (Figure 2.3 A), colorimetric-LAMP (Figure 2.3 B), and on a 2% agarose gel (Figure 2.3 C) performed for 60 min at 65 °C. Furthermore, we observed that targeting the N gene could detect the T7 RNA (2.33×10^9 to 2.33×10^6 per reaction) through the RT-LAMP with LFA (Figure 2.3 D), colorimetric-LAMP (Figure 2.3 E), and on a 2% agarose gel (Figure 2.3 F) performed for 60 min at 65 °C. To improve the efficiency of the RT-LAMP reaction for SARS-CoV-2 detection, we estimated the optimization of the primers and reaction time. The tests were assessed using the colorimetric-LAMP and RT-LAMP with LFA, for the LAMP primer set to target the S gene. We detected the T7 RNA (5.85×10^9 to 5.85×10^7 per reaction) through the RT-LAMP with LFA (Figure 2.4 A), colorimetric-LAMP (Figure 2.4 B), and on a 2% agarose gel (Figure 2.4 C) performed for the different reaction time of 30 or 60 min at 65 °C. The result showed T7 RNA detection under the same conditions. To further optimize the conditions for the S gene primers, loop primers were subsequently evaluated using synthesized T7 RNA through the RT-LAMP with LFA and colorimetric-LAMP assay. The RT-LAMP using only loop primers did not amplify the T7 RNA reaction of 60 min and at 65 °C (Figure 2.4 D - 2.4 F). These results indicate that the LAMP primer set with loop primers is more sensitive than the loop primers alone.

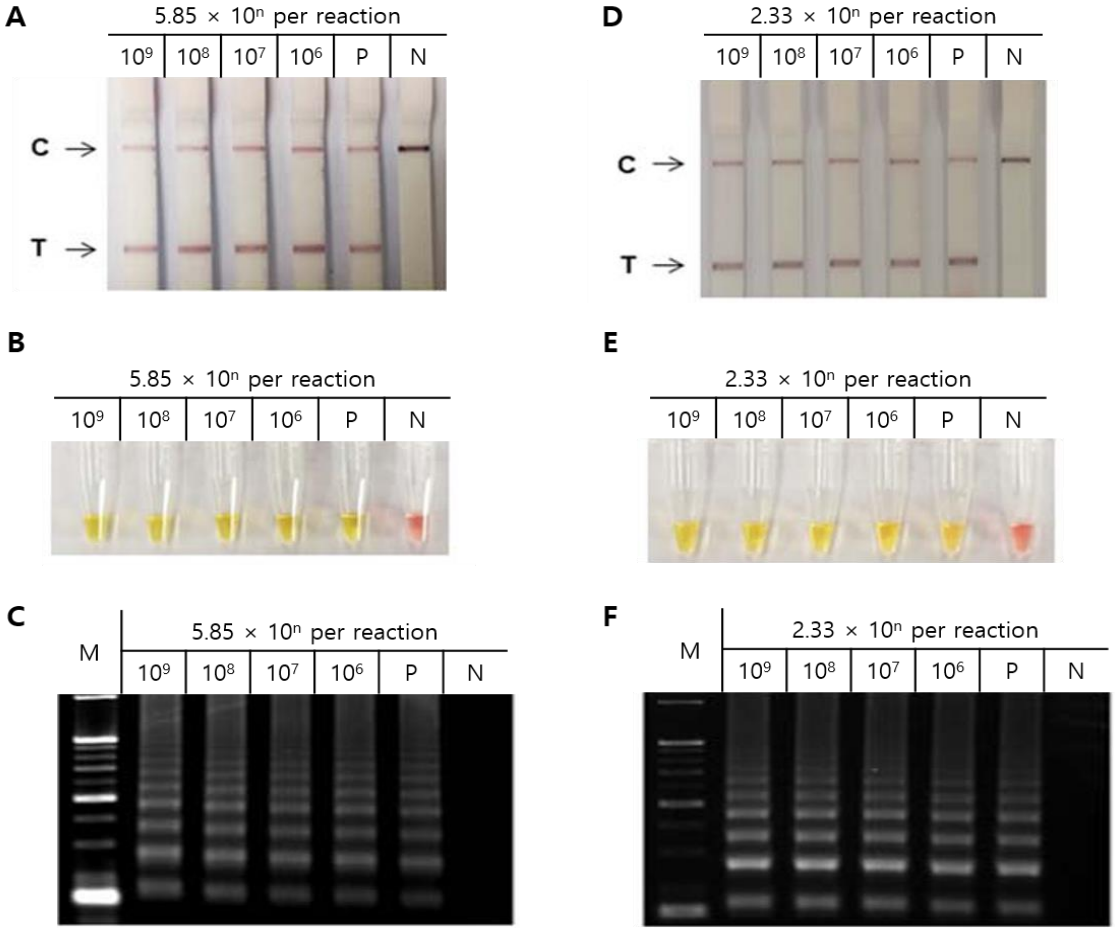

Figure 2.3 Application of RT-LAMP primers for SARS-CoV-2 detection.

(A-C) RT-LAMP with the S gene LAMP primers could detect the T7 RNA (5.85×10^9 to 5.85×10^6 per reaction). The reaction products were confirmed through (A) RT-LAMP with LFA, (B) colorimetric-LAMP, and (C) 2% agarose gel electrophoresis. (D-F) RT-LAMP with the N gene LAMP primers could detect the T7 RNA (2.33×10^9 to 2.33×10^6 per reaction). The reaction products were confirmed through (D) RT-LAMP with LFA, (E) colorimetric-LAMP, and (F) 2% agarose gel electrophoresis. All RT-LAMP reactions were performed at 65 °C for 60 min. S, spike; N, nucleocapsid; M, size marker; P, positive control; N, negative control; T, target; C, control.

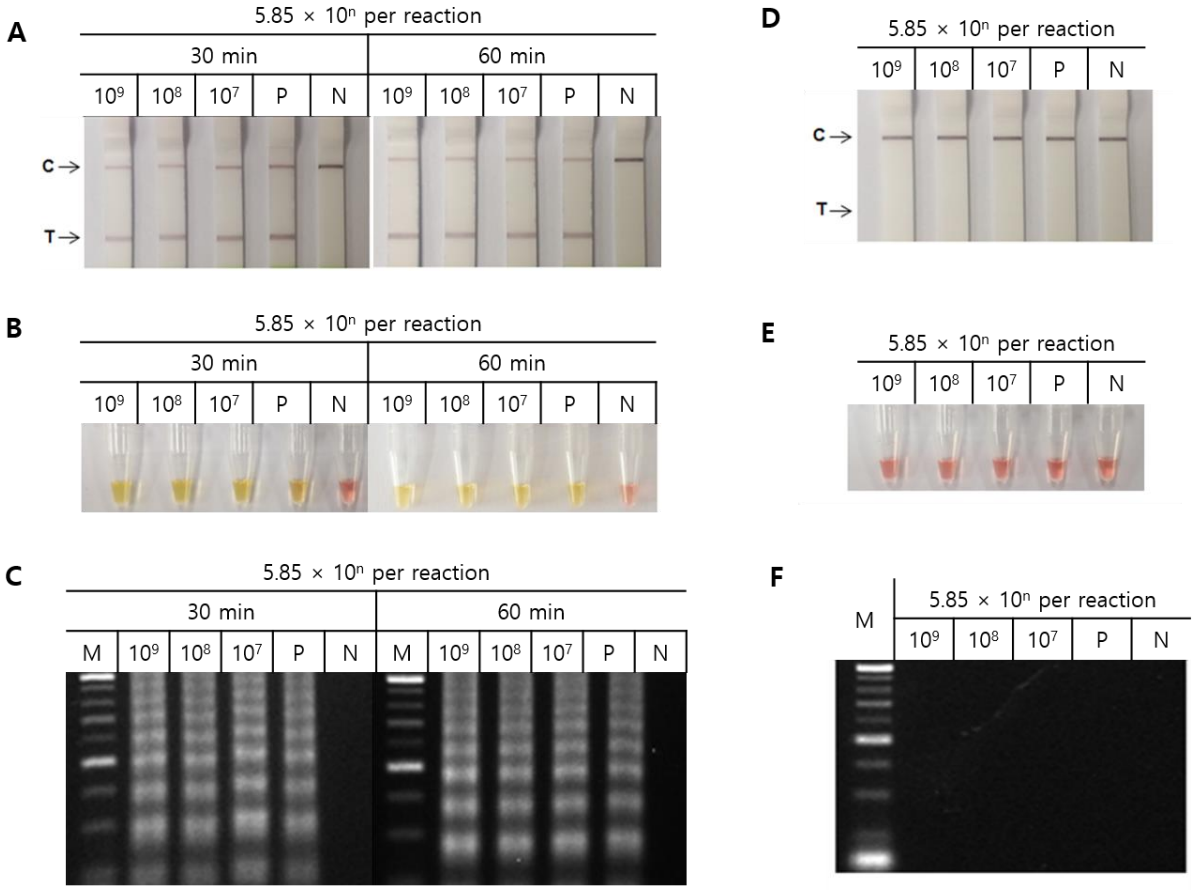

Figure 2.4 Optimization of RT-LAMP assay for SARS-CoV-2 detection.

RT-LAMP assay was performed using T7 RNA (5.85×10^9 to 5.85×10^7 per reaction) for the S gene of SARS-CoV-2. (A-C) Assessment of optimal reaction time of the RT-LAMP assay using a LAMP primer set comprising F3, B3, FIP, BIP, LF, and LB primers that recognize the S gene of SARS-CoV-2. RT-LAMP assay was performed for 30 or 60 min at 65 °C. The reaction products were confirmed through (A) RT-LAMP with LFA, (B) colorimetric RT-LAMP, and (C) 2% agarose gel electrophoresis. (D-F) Assessment of the sensitivity of the RT-LAMP assay by using only loop primers (LF and LB). The RT-LAMP assays were performed for 60 min at 65 °C. The reaction products were confirmed through (D) RT-LAMP with LFA, (E) colorimetric RT-LAMP, and (F) 2% agarose gel electrophoresis. M, size marker; P, positive control; N; negative control; T, target; C, control.

3.2.4. Validation of COVID-19 Molecular Diagnostic System on Human Specimens

To assess the clinical utility of the COVID-19 molecular diagnostics system, we performed 23 nasopharyngeal specimens including 8 patients with SARS-CoV-2 infection, 8 healthy participants, and 7 patients with other types of HCoV infection. The clinical specimens were processed for virus sample preparation using the DMP-PVDF platform. Then, the SARS-CoV-2 infection specimens were confirmed through the RT-LAMP with LFA and colorimetric RT-LAMP assays using the primer set targeting the S gene. We observed that the RT-LAMP with LFA could detect the 8 patients with SARS-CoV-2-positive specimens, as proved by a positive band on the LFA strip (Figure 2.5 A (up)). However, the colorimetric RT-LAMP assay could detect only 2 of the positive specimens (Figure 2.5 A (down)). These results show in the clinical specimens that the RT-LAMP with LFA is more sensitive than the colorimetric RT-LAMP. The 8 negative controls from the healthy participants did not test positive through either the RT-LAMP with LFA or colorimetric RT-LAMP assays (Figure 2.5 B). Furthermore, to validate the specificity of the RT-LAMP reaction for SARS-CoV-2 detection, we examined 7 nasopharyngeal specimens with other types including 5 patients with an HCoV-OC43 infection and 2 patients with an HCoV-229E infection. The RT-LAMP with LFA and colorimetric-LAMP assays using LAMP primers targeting the S gene were not amplified for any of the viral RNA from the other types of HCoV specimens (Figure 2.5 C). These results show that the RT-LAMP we designed has specificity for SARS-CoV-2. Therefore, the RT-LAMP with LFA can be used for the detection of COVID-19 with the naked-eye for POC testing. Thus, the rapid COVID-19 molecular diagnostic system can be a useful technique for the diagnosis of COVID-19 via effective virus enrichment and NAs extraction.

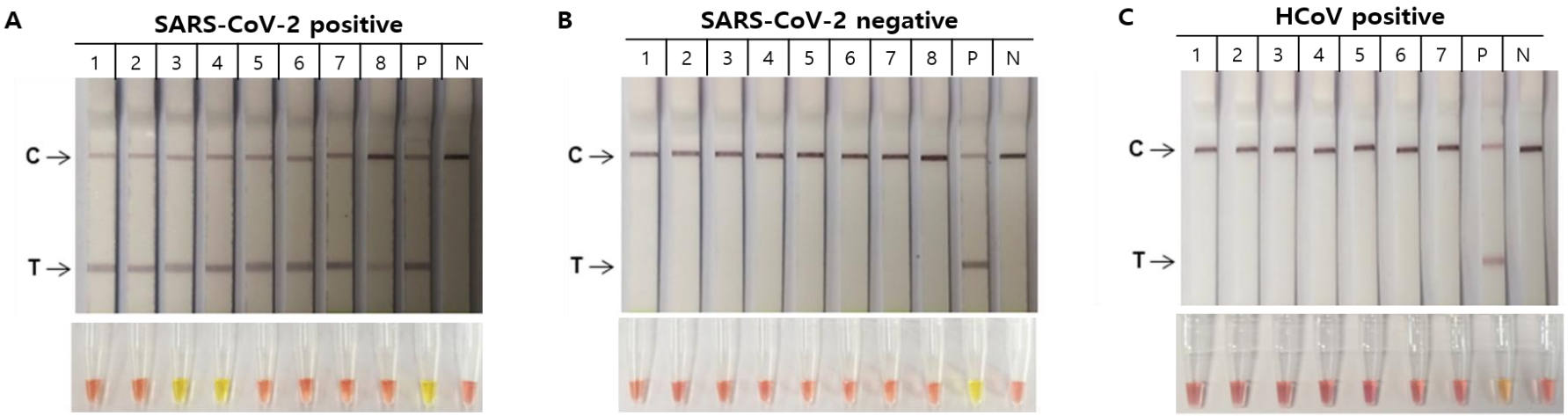

Figure 2.5 Clinical application of RT-LAMP and DMP-PVDF filter system on human specimens.

(A-C) Clinical application of the RT-LAMP and DMP-PVDF platform were analyzed 23 human nasopharyngeal specimens for the S gene of SARS-CoV-2 detection. (A) 8 patient specimens with SARS-CoV-2 infection were analyzed using DMP-PVDF platform by RT-LAMP with LFA (up) and colorimetric-LAMP (down). (B) 8 healthy participant specimens without SARS-CoV-2 infection were analyzed using DMP-PVDF platform by RT-LAMP with LFA (up) and colorimetric-LAMP (down). (C) Specificity of RT-LAMP assay for SARS-CoV-2 detection. RT-LAMP assay was performed using 7 clinical nasopharyngeal specimens from 5 HCoV-OC43 (lanes 1-5) and 2 HCoV-229E (lanes 6-7) patients for the S gene of SARS-CoV-2. The RT-LAMP assays were performed at 65 °C. RT-LAMP with LFA (up) and colorimetric-LAMP (down). P, positive control; N, negative control; T, target; C, control.

3.3 – Detection of mutant using HSSP

3.3.1. Principle and operation of the HSSP

The operating principles of HSSP are illustrated in Figure 3.1. HSSP was designed to overlap the target primer sequence, include a point mutation, and is modified with a C3 spacer at the 3'-end to prevent target DNA amplification by qPCR. When the target mutant sequence exists, the HSSP competitively attaches to the target mutant sequence, thereby preventing the primer from binding to the target DNA; subsequently, the HSSP attached DNA is not amplified. We designed HSSP was targeted at testing the detection efficiency of *KRAS* mutations that occur specifically in CRC; *G12D* (*GGT* → *GAT*) and *G13D* (*GGC* → *GAC*). In the case of wild-type with no *KRAS* mutations, the *KRAS* sequences were amplified; the HSSPs (*HSSP-G12D* and *HSSP-G13D*) could not block the amplification. If the *G12D* type mutation exists, the *KRAS* sequences were not amplified when using HSSP-G12D. However, the *KRAS* sequences were amplified due to do not block when using HSSP-G13D. Conversely, if the *G13D* type mutation exists, the *KRAS* sequences were not amplified when using HSSP-G13D.. However, the *KRAS* sequences were amplified due to do not block when using HSSP-G12D. For the decision of the mutation, we measured the differences in the C_t values between using HSSP-G12D and using HSSP-G13D based on the equation:

$$\Delta C_t \;=\; C_t\ (\mathrm{HSSP-G12D})\ -\ C_t\ (\mathrm{HSSP-G13D})$$

When the G12D mutation exists, ΔC_t is greater than 2. In the case of G13D mutation, ΔC_t is less than −2. In the wild-type sequence, the ΔC_t was 2 to −2. This method is a simple and easy approach that allows distinguishing the mutations within 1.5 h and is a rapid assay compared to the conventional used qPCR and sequencing methods.

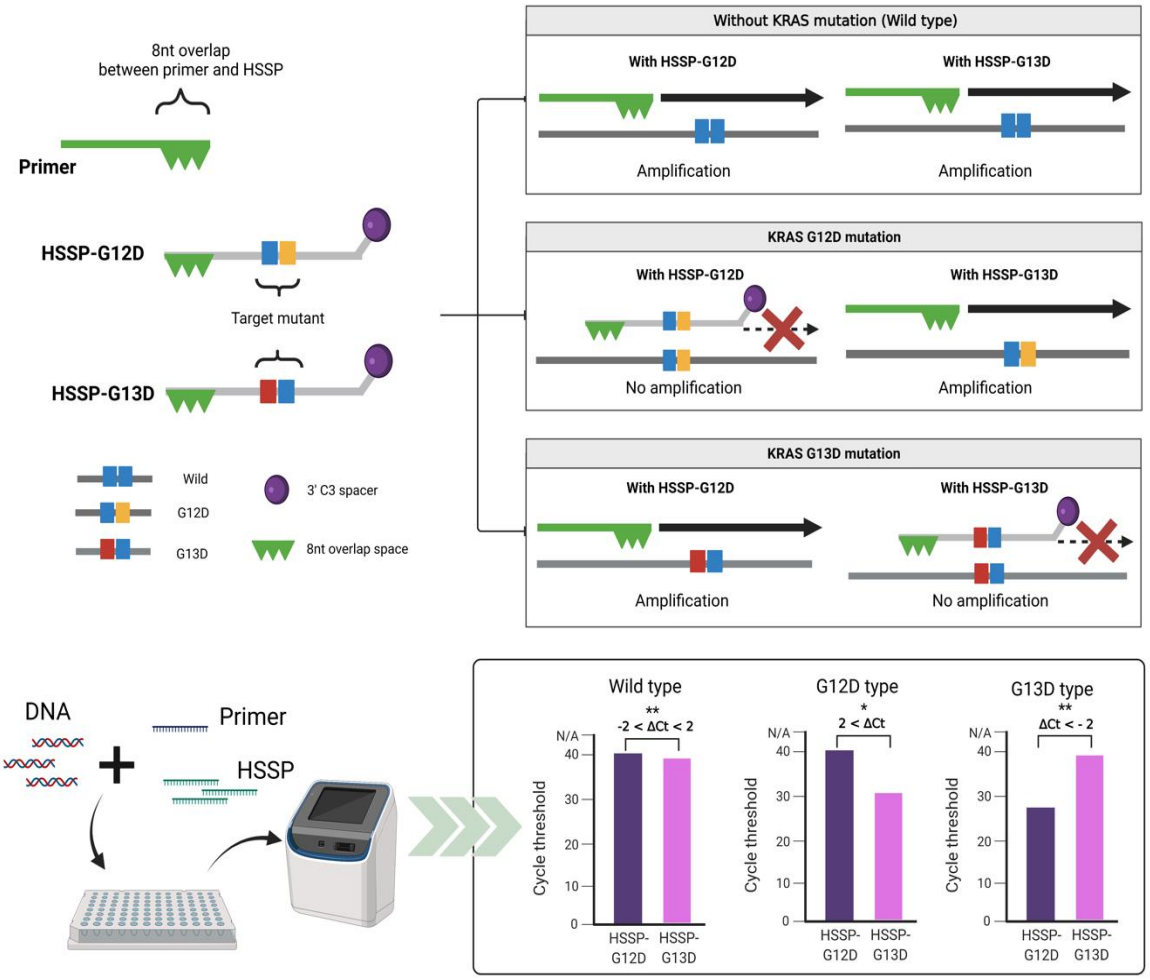

Figure 3.1 Schematic representation of the principle of HSSP.

The HSSP is designed to overlap with qPCR primers and contains single mutations. DNA of the target mutation sequence competitively attaches to the HSSP before the primer binds, which blocks amplification. In the case of sequences different from HSSP, the primer is attached and amplified. If you use HSSP for qPCR, mutants can be detected by mutation from the difference in the *Ct* values within 1.5 h. Calculation of the difference between the *Ct* values when each using HSSP-G12D and HSSP-G13D. If ΔC_t is higher than 2, it has the *G12D* type mutant; if ΔC_t is lower than −2, it has the *G13D* type mutant. A ΔC_t between 2 and −2 is considered wild-type.

3.3.2. Application and optimization of the HSSP

Prior to the use of HSSP, the efficiency of the primer was confirmed using qPCR. The limit of detection for primers was tested with either the *G12D* type mutant DNA or the *G13D* type mutant DNA or the wild-type DNA without mutations. It was confirmed that the limit of detection for the primers was 1×10^2 copies of the DNA from the three types (Figure 3.2 A). Next, to optimize for the concentration of HSSP, we used the serially diluted HSSP-G12D or HSSP-G13D (5–50 μM) for detection of the *KRAS* 12 or 13 mutation (Figure 3.2 B and 3.2 C). The Δ*Ct* value of qPCR was larger in high HSSP concentration at 25 μM and 50 μM, indicating that higher HSSP concentration could block the target DNA amplification by interfering with the binding of the primer to the target sequence. Although the *Ct* value with 50 μM HSSP was higher than that with 25 μM HSSP, the difference was not significant. Therefore, considering good stability, efficiency, and low cost, we selected 25 μM HSSP for HSSP-G12D (Figure 3.2 B) and HSSP-G13D (Figure 3.2 C).

After the optimization, we performed the direct sequencing and gel electrophoresis assays to confirm the utility of HSSP as a mutant amplified blocker (Figure 3.3). We used the direct sequencing assay to confirm heterozygous *G12D* and *G13D* mutations in AGS and HCT116 cell lines, respectively. When using HSSP-G12D in the AGS cell line, the *G12D* mutant signal was significantly reduced. Whereas, when using HSSP-G13D in the AGS cell line, the *G12D* mutant signal was emphasized by decreasing the wild-type signal (Figure 3.3 A). In the case of the *G13D* mutation in the HCT116 cell line, the *G13D* mutant signal was significantly reduced when HSSP-G13D was used. However, the *G13D* mutant signal was emphasized by decreasing the wild-type signal (Figure 3.3 B). The results from direct sequencing were similar to the results of the gel electrophoresis assay after conventional PCR (Figure 3.3 C). When we used HSSP-G12D and HSSP-G13D in the wild-type target, both HSSPs interfered

with the target DNA amplification. In the case of *G12D* and *G13D* cell lines, HSSP-G12D and HSSP-G13D interfered with the target mutant DNA amplification only (Figure 3.3 C). Therefore, the HSSPs specifically blocked the target mutant DNA amplification.

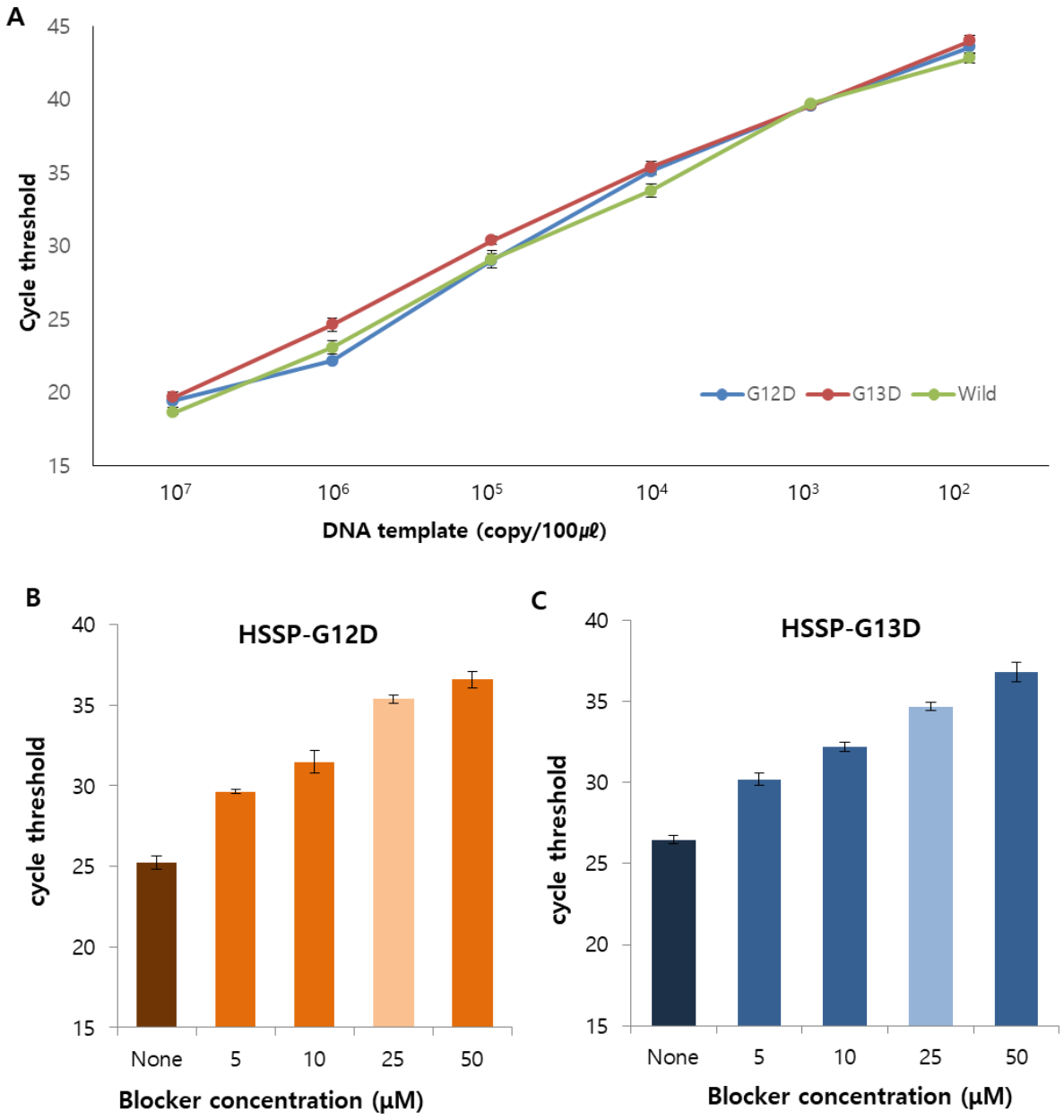

Figure 3.2 Application and optimization of the KRAS mutations primer and HSSP.

(A) The primer limit of detection is DNA 10^2 copies in three types when performed same way. (B-C) Efficiency of the HSSP depends on the concentration using (A) HSSP-G12D and (B) HSSP-G13D. It showed the largest difference at the highest concentration and the most stable value at 25 μM which is marked in light colors. The controls were not used HSSP and were displayed in darker colors. Data are presented as mean ± SD, based on at least three independent experiments.

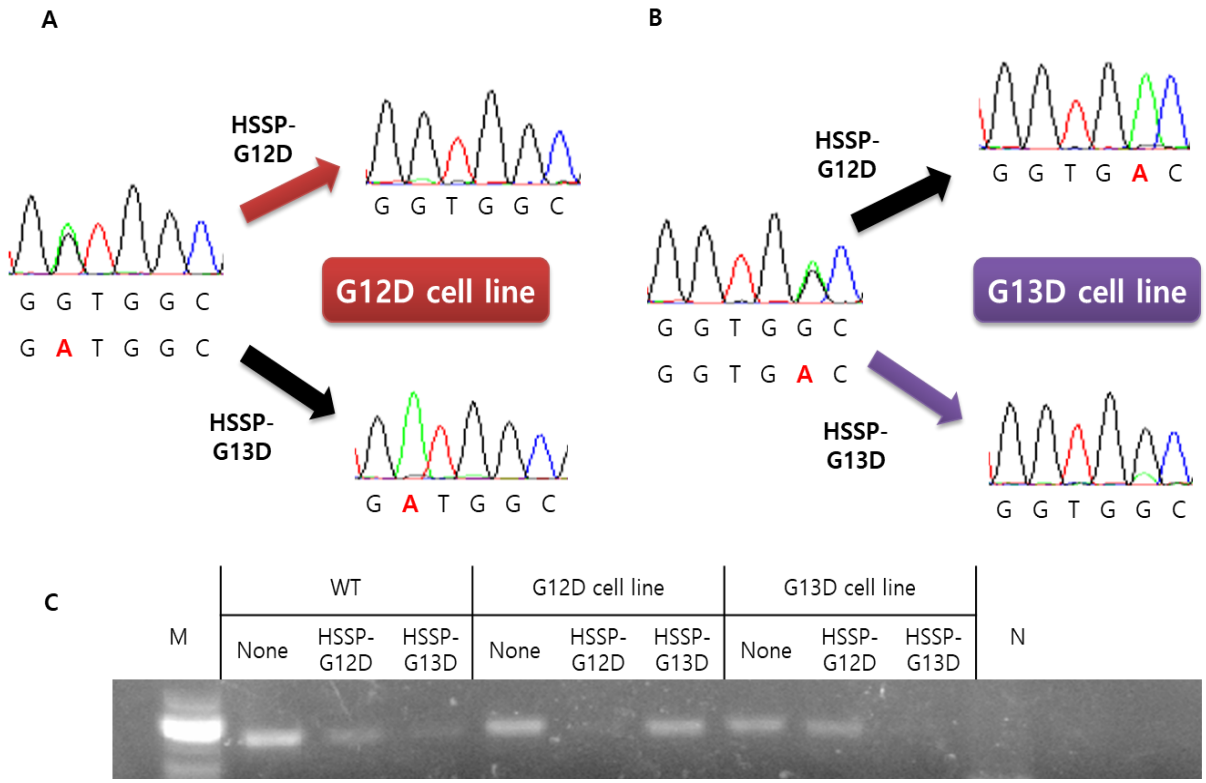

Figure 3.3 Application of blocking mutant amplification using HSSP.

(A-C) Operation of the HSSP was confirmed from direct sequencing and electrophoresis after end-point PCR. It shows that mutations were not amplified in DNA with the same sequence as the HSSP. (A–B) Direct sequencing results to confirm the operation of the HSSP on (A) G12D cell line and (B) G13D cell line. (C) Electrophoresis results after end-point PCR to confirm the operation of the HSSP. M, size marker; N; negative control

3.3.3. Detection limit of the KRAS mutation in mixed-cell populations

To check whether HSSP can distinguish the point mutation (*G12D* or *G13D*) in mixed-cell populations, we used serially diluted DNA samples from both AGS and HCT116 cell lines. Genomic DNA was obtained from the cell mixtures containing 0–100% of the mutant DNAs mixed with the wild-type DNA. When HSSP-G12D and HSSP-G13D were used to amplify the DNAs using qPCR, up to the mixture containing 10% of both *G12D* type (Figure 3.4 A) and *G13D* type (Figure 3.4 B) could be distinguished the mutant target. A previous report confirmed that PCR and direct sequencing could not detect the mutant allele in the mixed population containing >30% mutant templates [60]. However, the qPCR assay with HSSP could detect the mutant allele in the mixed samples containing 10% mutant templates in mixed sample populations. For accurate detection, we set an accurate standard for the ΔC_t value of qPCR. Using a wild-type DNA template, we checked from 10^7 copies to 10^3 copies and found that the ΔC_t value was 0.662, 1.29, 1.43, 0.84, and 0.47; thus, the maximum ΔC_t value was about 1.5. As a result, the average ΔC_t value in the wild-type is about 0.98, and the standard deviation is about 0.171. In addition, in the case of serial dilution, when the mutant template was 5%, the same pattern as the wild-type was shown. However, when the mutant template was 10%, the average ΔC_t value was 1.8 in *G12D* type and −2.4 in *G13D* type. Based on the case with a 10% mutant template, the mutation detection standard was determined. For more sensitive detection of the mutant DNAs, we performed a direct sequencing assay with HSSP. When direct sequencing was used to detect the *G12D* and *G13D* mutations, the mutant sequences could be distinguished at a 1% mutant template using HSSP (Figure 3.5). The wild-type strand cannot be amplified; only the mutation strand is emphasized. This confirmed that HSSP could detect nearly 1% of mutations using direct sequencing with both HSSP-G12D (Figure 3.5 A) and HSSP-G13D (Figure 3.5 B).

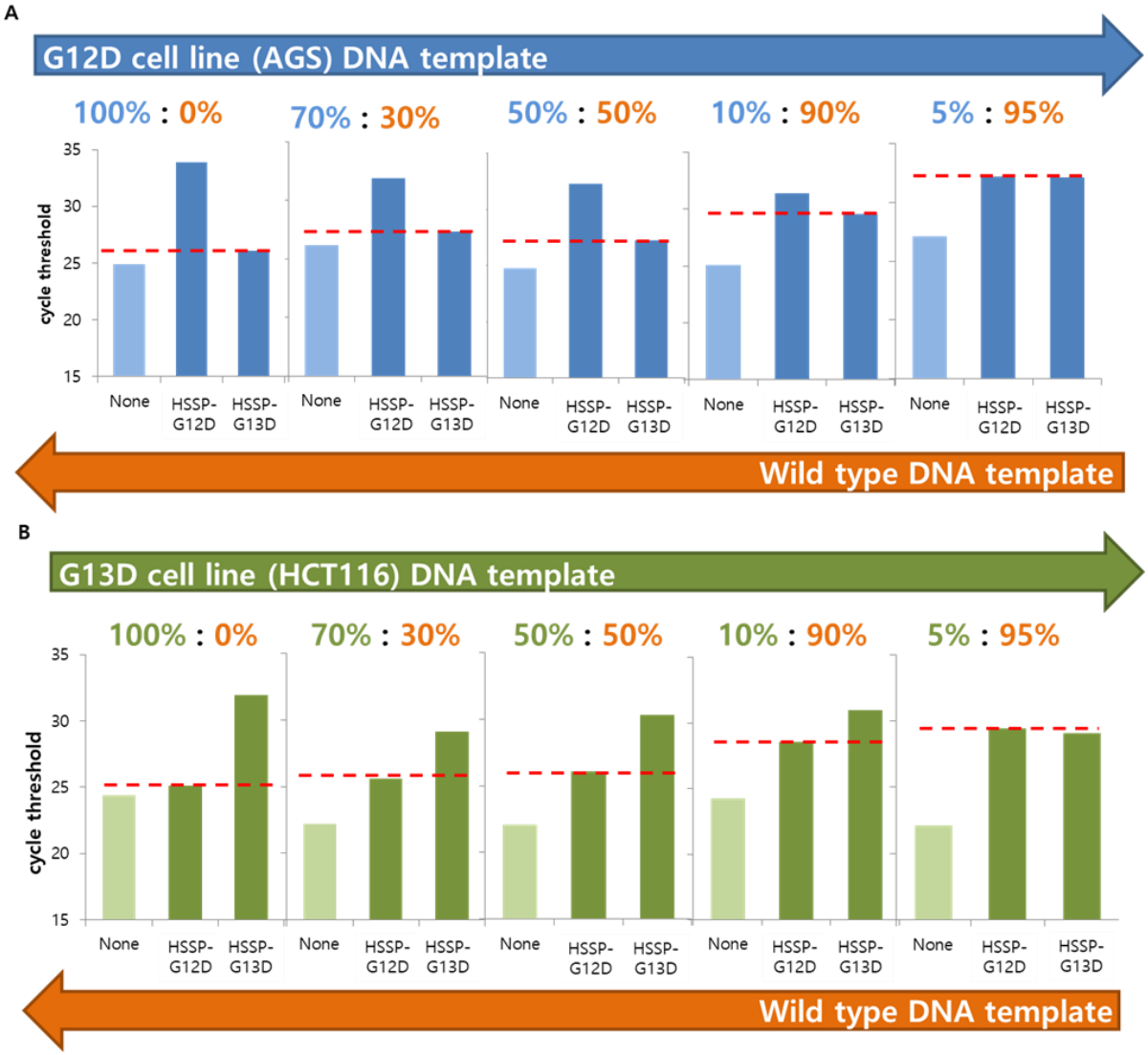

Figure 3.4 Analysis of the KRAS mutations with serially diluted mixed DNA template using HSSP with real-time PCR.

(A) *G12D* cell line (AGS) DNA template is by serial dilution with wild-type DNA template, and the detection limit of the mutant was checked. (B) *G13D* cell line (HCT116) DNA template is by serial dilution with wild-type DNA template, and the detection limit of the mutant was checked. In both cases, the value was indicated by a red line based on the case of using the non-target HSSP; the *Ct* value using HSSP-G13D in *G12D* mutation and the *Ct* value using HSSP-G12D in *G13D* mutation for visual confirmation of the difference in *Ct* values. Up to 10% is ΔC_t value, so it can be detected using HSSP with qPCR.

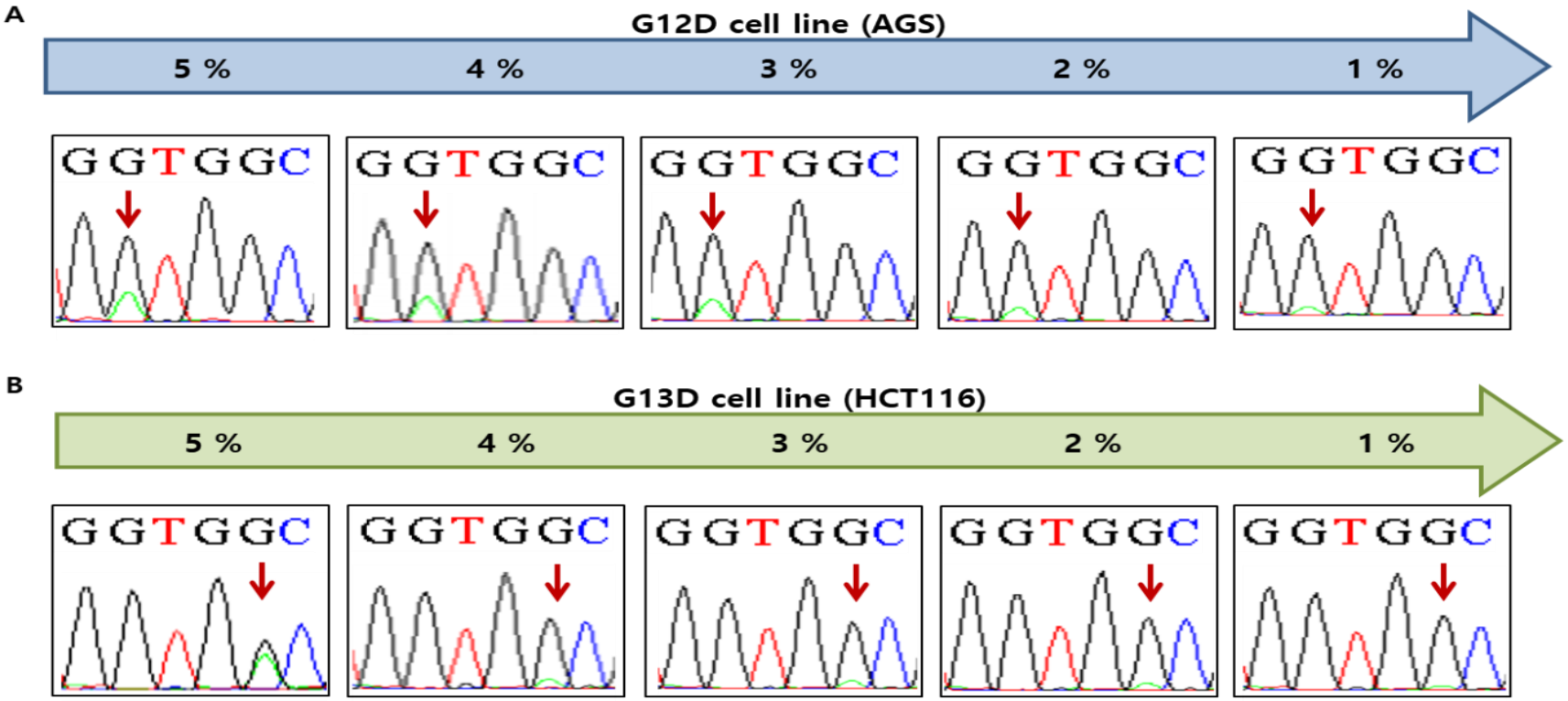

Figure 3.5 Analysis of the KRAS mutations with serially diluted mixed DNA template using HSSP with direct sequencing.

(**A**) *G12D* cell line (AGS) DNA template is by serial dilution with wild-type DNA template. When the AGS DNA template is used at less than 5%, it is possible to detect the mutant DNA templates at less than 1% if additional direct sequencing after qPCR with the HSSP-G13D. (**B**) *G13D* cell line (HCT116) DNA template is by serial dilution with wild-type DNA template. When the HCT116 DNA template is used at less than 5%, it is possible to detect the mutant template at less than 2% if additional direct sequencing after qPCR with the HSSP-G12D.

3.3.4. Sensitivity and specificity in clinical samples

To validate the clinical utility, we randomly selected 69 frozen tissue samples from patients with CRC treated at the BRC of Asan Medical Center. Among the 69 samples, 25 with the *G12D* mutation (36.2%), 25 with the *G13D* mutation (36.2%), and 19 with no mutation (27.6%) were examined at the BRC and were used as a reference [60]. Prior to confirming the utility in clinical samples, we checked performing HSSP in the representative data from four patients, including each two patients with the *G12D* mutation and the *G13D* mutation (Figure 3.6). Through this result, it was confirmed that HSSP works usefully even in clinical samples. By using HSSP-G12D and HSSP-G13D, the ΔC_t values showed the differences between the mutant and wild-types from all 69 clinical samples. For comparison, a direct sequencing assay was also performed with the same sample. From the results of HSSP with qPCR, 21 samples were detected as true positives (TP) and 4 as false negatives (FN) out of 25 samples with the *G12D* mutation. Among the 25 samples with the *G13D* mutation, 23 were detected as TP and 2 as FN. In the case of the 19 wild-type samples, 17 were detected as TP and 2 as FN. With the direct sequencing assay, 20 samples were detected as TP and 5 as false positives (FP) out of 25 samples with the *G12D* mutation. In 25 samples with the *G13D* mutation, 20 were detected as TP and 5 as FN. In the case of the wild-type samples, 19 out of 19 patients were detected as TP. Based on these results, the clinical specificity and sensitivity were calculated (Table 2). When we compared the clinical specificity and sensitivity of the two methods, HSSP with the qPCR assay showed higher sensitivity of 83.33% and 95% for *G12D* and *G13D* mutations, respectively. The specificity of HSSP with the qPCR assay was comparable to those of the direct sequencing assay. With these results, it was possible to see the high sensitivity and specificity of HSSP with the qPCR assay for mutation detection. Thus, by accelerating the diagnosis, the HSSP assay is expected to allow faster and more appropriate treatment for patients with cancer.

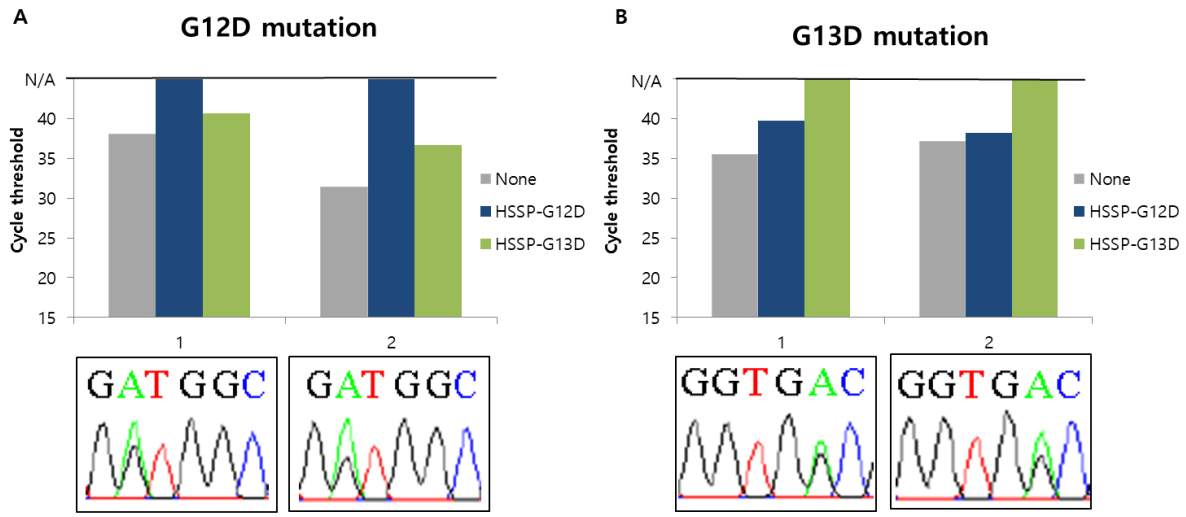

Figure 3.6 Application of the KRAS mutations detection in clinical samples.

Mutations in the clinical samples can be determined only by the HSSP with qPCR. The use of HSSP in the case of a target mutant type proved that there was a mutation if the mutation type was not amplified. Furthermore, through direct sequencing, it was confirmed that the result of using HSSP was correct. It was confirmed using clinical samples with (A) *G12D* mutation and (B) clinical samples with *G13D* mutation.

Table 2 Comparison of specificity and sensitivity in clinical samples of direct sequencing and the real-time PCR with HSSP

	HSSP with real-time PCR		**Direct Sequencing**	
KRAS	Sensitivity (95% CI)	Specificity (95% CI)	Sensitivity (95% CI)	Specificity (95% CI)
G12D	83.33% (62.62% to 95.26%)	97.3% (85.84% to 99.93%)	80.00% (59.30% to 93.17%)	100% (89.72% to 100.00%)
G13D	95% (75.13% to 99.87%)	92.68% (80.08% to 98.46%)	80.00% (59.30% to 93.17%)	97.06% (84.67% to 99.93%)
WT	88.24% (63.56% to 98.54%)	93.18% (81.34% to 98.57%)	100% (82.35% to 100.00%)	82.00% (68.56% to 91.42%)

4. DISCUSSION

Rapid and accurate molecular diagnostic methods have been studied in the field of biomedical engineering for decades. However, there are still many challenges with the sample preparation method for molecular diagnosis. The complicated procedure is time-consuming and expensive. In addition, initial diagnosis is difficult because there is no technology that can concentrate pathogens at low concentrations. In this study, a new sample preparation technology was developed to solve these limitations. The DMP-PVDF platform is simple and cheap, and can only be used by hand without the need for instruments. It is also important to concentrate in samples with low concentrations of bacteria, in which the DMP-PVDF platform is no capacity limit, so large scale of samples can be used to enrichment more bacteria. This platform provides a simple, reliable, cost-effective, and sensitive for use with small to large volumes of clinical samples.

Using a DMP-PVDF platform with these advantages, this study reports a rapid COVID-19 molecular diagnostic system that can be easily operated using portable materials without highly trained professionals or complex procedures. Previous studies have reported that isothermal amplification techniques can be used for SARS-CoV-2 detection in RNAs of clinical samples such as nasopharynx or pharynx swabs. However, the diagnostic analysis developed in these studies has limitations associated with kit and centrifugation steps [23, 69-71], requiring sophisticated instruments and special reagents such as fluorescent dyes [24, 69-71]. We demonstrate a diagnostic system combining simple pathogen enrichment methods including RT-LAMP and DMP-PVDF filters for quick and accurate detection of SARS-CoV-2. Using the system, we validate clinical utility in 23 nasopharyngeal clinical samples and establish improved sensitivity and specificity. Furthermore, using this proposed system for pathogen enrichment, amplification, and detection of viral RNA does not require expensive

reagents. Based on these experimental results, we compared the proposed technique with the COVID-19 diagnostic kits currently commercialized (Table 3). Many products are commercialized using real-time PCR and are used worldwide. However, these products do not include the sample preparation steps. So, it takes 50-70 min for the detection step, and it takes more time if includes the sample preparation steps. This clearly shows the advantages of our technology, which takes 60 min, including the sample preparation steps. In addition, rapid diagnosis, which is diagnosed with an antigen or antibody, can be diagnosed easily and quickly. It is difficult to diagnose in the early stages of symptoms. Compared to other rapid diagnostic methods, the proposed technique can be detected even at the early stages of the symptom, and it can be diagnosed at a low price of $10.148 per sample with a short time of 60 min from sample preparation to detection. Thus, the proposed technique might be used for point-of-care diagnosis. Therefore, our results suggest that RT-LAMP and DMP-PVDF filter combination systems can be used for limited resource settings, POCs, or for diagnostic purposes at home. In addition, the cost is much lower than a PCR-based hospital test. The ultimate purpose of this proposed system is the early diagnosis of COVID-19 made directly to individuals at home or POC without sophisticated tools. Consequently, the system described in this study provides a simple, sensitive, convenient, efficient, and affordable strategy that can be easily applied to the diagnosis of emerging infectious diseases such as COVID-19.

In addition to this field diagnosis, several molecular diagnostic methods for detecting mutations have been reported. NGS [72], the most widely used method, is expensive and time-consuming, and other PCR-based methods have limitations that vary in efficiency from commercial kit to commercial kit, or require additional expensive equipment [49, 51, 52, 73, 74]. This takes a shorter time than the direct sequencing assay, which takes at least several days to deliver the result. In addition, in terms of cost, it is less than $2 per sample, which is

cheaper than other methods. Differences in Ct values can easily be checked using this analysis technique, so it can be easily used to detect other mutations. The LOD of HSSP (5–10% of mutant allele) is higher than those of other assays, such as qPCR and direct sequencing (≥30% of mutant allele). Hence, HSSP with qPCR is highly useful for the detection of hot spot mutations in clinical specimens instead of any sequencing assay. When 69 clinical samples were examined, the clinical sensitivity of HSSP with the qPCR assay was superior to that of the direct sequencing assay (Table 2). These results show more accuracy in the diagnosis of wild type that does not use Anti-EGFR MoAb, so it is expected that faster and more appropriate treatment will be available for wild type. In addition, this method is expected to be able to detect different mutations by designing different HSSPs, enabling various applications.

Table 3 Summary of the commercialized products of COVID-19 detection.

Name	Category	Types of clinical specimens	Target	Available readouts	Time	LOD
Rapid COVID-19 diagnostic system	Molecular	Nasopharyngeal swab	S or N gene	LFA, Colorimetric RT-LAMP	40-60 min	5 copies /reaction
Allplex 2019-nCoV Assay		Sputum, Nasal swab, etc.	E, RdRp or N gene	Bio-rad CFX96	70min	100 copies/ reactions
STANDARD M nCoV Real-Time Detection kit		Sputum, Nasal swab, etc.	E or ORF1 gene	Roche Lightcycler 480	50-55min	0.5 - 0.125 copies /μL
Standard Q COVID-19 Ag Test	Antigen	Nasopharyngeal swab	Nucleocapsid protein	LFA	15-30 min	1.12 x 10^2 PFU/ml
Humasis COVID-19 IgG/IgM Test	Antibody	Whole blood, Serum, Plasma	IgG	LFA	10-15min	1:50 dilution ratio

5. CONCLUSION

This study presented a new platform that demonstrates the potential for point-of-care tests and a new method for mutant detection. Sample preparation techniques using the DMP-PVDF platform demonstrate that they can proceed quickly and simply. Above all, the process is carried out only with hands without instruments so, it is suitable for POC tests in a limited environment. In addition, naked-eye detection using the isothermal PCR technique is integrated with the DMP-PVDF platform to provide simpler, more sensitive, convenient, efficient, and reasonable techniques. This showed a very high possibility for the POC testing. Mutant detection techniques using HSSP have provided more sensitive, faster, and cheaper that can be easily applied than the gold standard method of sequencing. Therefore, further research is needed to confirm the clinical usefulness of molecular diagnostic systems using a large cohort of human samples.

These proposed techniques in this study have been demonstrated separately. Thus, the integration of the sample preparation step and detection step as proposed techniques may provide in various disease diagnoses POC tests as well as in many clinical applications such as customized treatment, and cancer monitoring. In addition, it has possibilities in many fields such as biological research, and animal healthcare, environmental pollution monitoring.

6. REFERENCES

1. Hong, K.H., et al., *Guidelines for Laboratory Diagnosis of Coronavirus Disease 2019 (COVID-19) in Korea.* Annals of Laboratory Medicine, 2020. **40**(5): p. 351-360.
2. Chakraborty, I. and P. Maity, *COVID-19 outbreak: Migration, effects on society, global environment and prevention.* Sci Total Environ, 2020. **728**: p. 138882.
3. Miller, I.F., et al., *Disease and healthcare burden of COVID-19 in the United States.* Nat Med, 2020. **26**(8): p. 1212-1217.
4. Kramer, V., et al., *Subjective burden and perspectives of German healthcare workers during the COVID-19 pandemic.* Eur Arch Psychiatry Clin Neurosci, 2021. **271**(2): p. 271-281.
5. Arons, M.M., et al., *Presymptomatic SARS-CoV-2 Infections and Transmission in a Skilled Nursing Facility.* N Engl J Med, 2020. **382**(22): p. 2081-2090.
6. Mizumoto, K., et al., *Estimating the asymptomatic proportion of coronavirus disease 2019 (COVID-19) cases on board the Diamond Princess cruise ship, Yokohama, Japan, 2020.* Euro Surveill, 2020. **25**(10).
7. Padhi, A., et al., *Laboratory Diagnosis of Novel Coronavirus Disease 2019 (COVID-19) Infection*, in *Coronavirus Disease 2019 (COVID-19): Epidemiology, Pathogenesis, Diagnosis, and Therapeutics*, S.K. Saxena, Editor. 2020, Springer Singapore: Singapore. p. 95-107.
8. Han, S., et al., *Rapid Diagnosis of Coronavirus by RNA-Directed RNA Transcription Using an Engineered RNA-based Platform.* Nano Letters, 2021. **21**(1): p. 462-468.
9. Noh, G.S., et al., *Multi-Sample Preparation Assay for Isolation of Nucleic Acids Using Bio-Silica with Syringe Filters.* Micromachines, 2020. **11**(9).
10. Jung, J.H., et al., *Combination of multiplex reverse-transcription loop-mediated isothermal amplification with an immunochromatographic strip for subtyping influenza A virus.* Analytica Chimica Acta, 2015. **853**: p. 541-547.
11. Lagier, J.C., et al., *Current and Past Strategies for Bacterial Culture in Clinical Microbiology.* Clinical Microbiology Reviews, 2015. **28**(1): p. 208-236.
12. Liu, H., et al., *Trends and challenges of nanotechnology in self-test at home.* Trac-

Trends in Analytical Chemistry, 2021. **144**.

13. Jang, Y.O., et al., *Fecal microbial transplantation and a high fiber diet attenuates emphysema development by suppressing inflammation and apoptosis.* Experimental and Molecular Medicine, 2020. **52**(7): p. 1128-1139.

14. Hanff, P.A., et al., *Purification of Treponema-Pallidum, Nichols Strain, by Percoll Density Gradient Centrifugation.* Sexually Transmitted Diseases, 1984. **11**(4): p. 275-286.

15. Stevens, K.A. and L.A. Jaykus, *Bacterial separation and concentration from complex sample matrices: A review.* Critical Reviews in Microbiology, 2004. **30**(1): p. 7-24.

16. Corman, V.M., et al., *Detection of 2019 novel coronavirus (2019-nCoV) by real-time RT-PCR.* Euro Surveill, 2020. **25**(3).

17. Wozniak, A., et al., *A simple RNA preparation method for SARS-CoV-2 detection by RT-qPCR.* Sci Rep, 2020. **10**(1): p. 16608.

18. Pfefferle, S., et al., *Evaluation of a quantitative RT-PCR assay for the detection of the emerging coronavirus SARS-CoV-2 using a high throughput system.* Eurosurveillance, 2020. **25**(9): p. 18-22.

19. Pillonel, T., et al., *Letter to the editor: SARS-CoV-2 detection by real-time RT-PCR.* Eurosurveillance, 2020. **25**(21): p. 33-34.

20. Mackay, I.M., K.E. Arden, and A. Nitsche, *Real-time PCR in virology.* Nucleic Acids Res, 2002. **30**(6): p. 1292-305.

21. Drosten, C., et al., *Rapid detection and quantification of RNA of Ebola and Marburg viruses, Lassa virus, Crimean-Congo hemorrhagic fever virus, Rift Valley fever virus, dengue virus, and yellow fever virus by real-time reverse transcription-PCR.* J Clin Microbiol, 2002. **40**(7): p. 2323-30.

22. Wan, Z., et al., *A Melting Curve-Based Multiplex RT-qPCR Assay for Simultaneous Detection of Four Human Coronaviruses.* Int J Mol Sci, 2016. **17**(11).

23. Broughton, J.P., et al., *CRISPR-Cas12-based detection of SARS-CoV-2.* Nat Biotechnol, 2020. **38**(7): p. 870-874.

24. Wang, R., et al., *opvCRISPR: One-pot visual RT-LAMP-CRISPR platform for SARS-*

cov-2 detection. Biosens Bioelectron, 2021. **172**: p. 112766.

25. Jiang, M.H., et al., *Development and Validation of a Rapid, Single-Step Reverse Transcriptase Loop-Mediated Isothermal Amplification (RT-LAMP) System Potentially to Be Used for Reliable and High-Throughput Screening of COVID-19.* Frontiers in Cellular and Infection Microbiology, 2020. **10**.

26. Wong, Y.P., et al., *Loop-mediated isothermal amplification (LAMP): a versatile technique for detection of micro-organisms.* Journal of Applied Microbiology, 2018. **124**(3): p. 626-643.

27. Parida, M., et al., *Loop mediated isothermal amplification (LAMP): a new generation of innovative gene amplification technique; perspectives in clinical diagnosis of infectious diseases.* Reviews in Medical Virology, 2008. **18**(6): p. 407-421.

28. Rabe, B.A. and C. Cepko, *SARS-CoV-2 detection using isothermal amplification and a rapid, inexpensive protocol for sample inactivation and purification.* Proceedings of the National Academy of Sciences of the United States of America, 2020. **117**(39): p. 24450-24458.

29. Bruning, A.H.L., et al., *Rapid Tests for Influenza, Respiratory Syncytial Virus, and Other Respiratory Viruses: A Systematic Review and Meta-analysis.* Clin Infect Dis, 2017. **65**(6): p. 1026-1032.

30. Tanner, N.A., Y.H. Zhang, and T.C. Evans, *Visual detection of isothermal nucleic acid amplification using pH-sensitive dyes.* Biotechniques, 2015. **58**(2): p. 59-68.

31. Lee, D., et al., *Simple and Highly Sensitive Molecular Diagnosis of Zika Virus by Lateral Flow Assays.* Analytical Chemistry, 2016. **88**(24): p. 12272-12278.

32. Jemal, A., et al., *Global Cancer Statistics.* Ca-a Cancer Journal for Clinicians, 2011. **61**(2): p. 69-90.

33. Bray, F., et al., *Global cancer statistics 2018: GLOBOCAN estimates of incidence and mortality worldwide for 36 cancers in 185 countries.* Ca-a Cancer Journal for Clinicians, 2018. **68**(6): p. 394-424.

34. Siegel, R.L., et al., *Colorectal cancer statistics, 2020.* Ca-a Cancer Journal for Clinicians, 2020. **70**(3): p. 145-164.

35. Xie, Y.H., Y.X. Chen, and J.Y. Fang, *Comprehensive review of targeted therapy for*

colorectal cancer. Signal Transduction and Targeted Therapy, 2020. **5**(1).

36. Biller, L.H. and D. Schrag, *Diagnosis and Treatment of Metastatic Colorectal Cancer: A Review.* Jama-Journal of the American Medical Association, 2021. **325**(7): p. 669-685.

37. Phipps, A.I., et al., *KRAS-mutation status in relation to colorectal cancer survival: the joint impact of correlated tumour markers.* British Journal of Cancer, 2013. **108**(8): p. 1757-1764.

38. Imamura, Y., et al., *Specific Mutations in KRAS Codons 12 and 13, and Patient Prognosis in 1075 BRAF Wild-Type Colorectal Cancers.* Clinical Cancer Research, 2012. **18**(17): p. 4753-4763.

39. Timar, J. and K. Kashofer, *Molecular epidemiology and diagnostics of KRAS mutations in human cancer.* Cancer and Metastasis Reviews, 2020. **39**(4): p. 1029-1038.

40. Karapetis, C.S., et al., *K-ras mutations and benefit from cetuximab in advanced colorectal cancer.* New England Journal of Medicine, 2008. **359**(17): p. 1757-1765.

41. Walther, A., et al., *Genetic prognostic and predictive markers in colorectal cancer.* Nature Reviews Cancer, 2009. **9**(7): p. 489-499.

42. Molinari, F., et al., *Increased Detection Sensitivity for KRAS Mutations Enhances the Prediction of Anti-EGFR Monoclonal Antibody Resistance in Metastatic Colorectal Cancer.* Clinical Cancer Research, 2011. **17**(14): p. 4901-4914.

43. Tougeron, D., et al., *Effect of low-frequency KRAS mutations on the response to anti-EGFR therapy in metastatic colorectal cancer.* Annals of Oncology, 2013. **24**(5): p. 1267-1273.

44. Wu, L.R., et al., *Multiplexed enrichment of rare DNA variants via sequence-selective and temperature-robust amplification.* Nature biomedical engineering, 2017. **1**: p. 714-723.

45. Lai, W., et al., *Circularized blocker-displacement amplification for multiplex detection of rare DNA variants.* Chemical Communications, 2020. **56**(82): p. 12331-12334.

46. Yamin, W. and C. Zhong, *Mutation detection and molecular targeted tumor therapies.*

STEMedicine, 2020. **1**(1).

47. Su, N., et al., *Sensitive and selective detections of codon 12 and 13 KRAS mutations in a single tube using modified wild-type blocker.* Clinica Chimica Acta, 2019. **494**: p. 123-131.

48. Dufort, S., M.J. Richard, and F. de Fraipont, *Pyrosequencing method to detect KRAS mutation in formalin-fixed and paraffin-embedded tumor tissues.* Analytical Biochemistry, 2009. **391**(2): p. 166-168.

49. Vivancos, A., et al., *Comparison of the Clinical Sensitivity of the Idylla Platform and the OncoBEAM RAS CRC Assay for KRAS Mutation Detection in Liquid Biopsy Samples.* Scientific Reports, 2019. **9**.

50. Holm, M., et al., *Detection of KRAS mutations in liquid biopsies from metastatic colorectal cancer patients using droplet digital PCR, Idylla, and next generation sequencing.* Plos One, 2020. **15**(11).

51. Dong, L.H., et al., *Evaluation of droplet digital PCR and next generation sequencing for characterizing DNA reference material for KRAS mutation detection.* Scientific Reports, 2018. **8**.

52. Didelot, A., et al., *Competitive allele specific TaqMan PCR for KRAS, BRAF and EGFR mutation detection in clinical formalin fixed paraffin embedded samples.* Experimental and Molecular Pathology, 2012. **92**(3): p. 275-280.

53. Chubarov, A.S., et al., *Allele-Specific PCR for KRAS Mutation Detection Using Phosphoryl Guanidine Modified Primers.* Diagnostics, 2020. **10**(11): p. 872.

54. Jang, Y.O., et al., *Dimethyl 3,3'-dithiobispropionimidate-functionalized diatomaceous earth particles for efficient biomolecule separation.* Sci Rep, 2020. **10**(1): p. 15592.

55. Liu, H., et al., *Large Instrument- and Detergent-Free Assay for Ultrasensitive Nucleic Acids Isolation via Binary Nanomaterial.* Anal Chem, 2018. **90**(8): p. 5108-5115.

56. Jin, C.E., et al., *Simple and label-free pathogen enrichment via homobifunctional imidoesters using a microfluidic (SLIM) system for ultrasensitive pathogen detection in various clinical specimens.* Biosensors & Bioelectronics, 2018. **111**: p. 66-73.

57. Shin, Y., et al., *Dimethyl adipimidate/Thin film Sample processing (DTS); A simple, low-cost, and versatile nucleic acid extraction assay for downstream analysis.*

Scientific Reports, 2015. **5**.

58. Vestheim, H. and S.N. Jarman, *Blocking primers to enhance PCR amplification of rare sequences in mixed samples - a case study on prey DNA in Antarctic krill stomachs.* Frontiers in Zoology, 2008. **5**.

59. Dames, S., et al., *Characterization of aberrant melting peaks in unlabeled probe assays.* Journal of Molecular Diagnostics, 2007. **9**(3): p. 290-296.

60. Jin, C.E., et al., *Rapid and accurate detection of KRAS mutations in colorectal cancers using the isothermal-based optical sensor for companion diagnostics.* Oncotarget, 2017. **8**(48): p. 83860-83871.

61. Bhutta, Z.A., *Current concepts in the diagnosis and treatment of typhoid fever.* Bmj-British Medical Journal, 2006. **333**(7558): p. 78-82b.

62. Saraswathi, M.S.A., et al., *BSA and humic acid separation from aqueous stream using polydopamine coated PVDF ultrafiltration membranes.* Journal of Environmental Chemical Engineering, 2017. **5**(3): p. 2937-2943.

63. Bai, H.L., et al., *Preparation and characterization of poly(vinylidene fluoride) composite membranes blended with nano-crystalline cellulose.* Progress in Natural Science-Materials International, 2012. **22**(3): p. 250-257.

64. Lu, X.M., et al., *Anti-fouling membranes by manipulating surface wettability and their anti-fouling mechanism.* Desalination, 2017. **413**: p. 127-135.

65. Al-Gharabli, S., et al., *Biomimetic hybrid membranes with covalently anchored chitosan - Material design, transport and separation.* Desalination, 2020. **491**.

66. Gu, S., et al., *Preparation and Characterization of Poly(vinylidene fluoride)/Sulfonated Poly(phthalazinone ether sulfone ketone) Blends for Proton Exchange Membrane.* Journal of Applied Polymer Science, 2010. **116**(2): p. 852-860.

67. Zhang, Y., et al., *Electrospun porous poly(tetrafluoroethylene-co-hexafluoropropylene-co-vinylidene fluoride) membranes for membrane distillation.* Rsc Advances, 2017. **7**(89): p. 56183-56193.

68. Zhou, Y.F., et al., *Preparation of hyperbranched polymer films grafted on self-assembled monolayers.* Journal of the American Chemical Society, 1996. **118**(15): p. 3773-3774.

69. Patchsung, M., et al., *Clinical validation of a Cas13-based assay for the detection of SARS-CoV-2 RNA.* Nat Biomed Eng, 2020. **4**(12): p. 1140-1149.

70. Ding, X., et al., *Ultrasensitive and visual detection of SARS-CoV-2 using all-in-one dual CRISPR-Cas12a assay.* Nature Communications, 2020. **11**(1).

71. Huang, Z., et al., *Ultra-sensitive and high-throughput CRISPR-p owered COVID-19 diagnosis.* Biosensors & Bioelectronics, 2020. **164**.

72. Newman, A.M., et al., *An ultrasensitive method for quantitating circulating tumor DNA with broad patient coverage.* Nature Medicine, 2014. **20**(5): p. 552-558.

73. Demuth, C., et al., *Measuring KRAS Mutations in Circulating Tumor DNA by Droplet Digital PCR and Next-Generation Sequencing.* Translational Oncology, 2018. **11**(5): p. 1220-1224.

74. Diehl, F., et al., *Analysis of mutations in DNA isolated from plasma and stool of colorectal cancer patients.* Gastroenterology, 2008. **135**(2): p. 489-498.

7. ABSTRACT (KOREA)

박테리아와 바이러스에 의한 감염병은 전 세계적으로 많은 사람들에게 위험을 주며, 심각할 경우에는 경제적 손실을 포함한 문제를 일으킬 수 있습니다. 최근 중증급성호흡기증후군(SARS-CoV-2)로 인한 코로나바이러스(COVID-19) 대유행은 빠르게 확산되어 전 세계의 의료 시스템과 경제적인 커뮤니티에 심각한 영향을 주었습니다. 따라서 감염병의 추가적인 확산을 방지하고 의료시설 및 진단시설의 부담을 줄여주며 빠른 치료를 보장하기 위해서는 감염병에 대한 정확하고 신속하며 진단이 매우 중요합니다. 질병의 빠르면서 정확한 분자 진단을 위한 다양한 기술의 개발되고 있습니다. 그럼에도 불구하고, 몇 가지 해결해야 하는 단점은 계속 존재하고 있습니다. 예를 들어, 병원균의 농도가 매우 낮은 임상 샘플과 복잡한 과정을 필요로 하는 기구들, 시간이 많이 걸리며 전문적인 인력을 필요로 한다는 문제점이 아직까지 있습니다. 이러한 문제점들은 해결하기 위해서 PVDF 주사기 필터를 사용하여 병원체 농축과 핵산 추출을 할 수 있는 새로운 방법과 임상 검체에서 정확한 검출을 수행하는 데 사용할 수 있는 민감한 검출 기술들을 이용한 새로운 질병 진단 분석을 개발했습니다.

검체 전처리 단계를 위해, 우리는 환자에게서 채취한 시료에서 박테리아나 바이러스를 농축 및 핵산 추출을 위해 상용화된 제품인 PVDF 주사기 필터를 이용한 방법을 개발했습니다. PVDF 주사기 필터에, DMP라는 가교결합 역할을 해주는 HI 시약 중 하나의 물질을 사용하였습니다. DMP는 핵산의 아민 그룹과 반응하여 아미딘 결합을 형성하고 정전 결합을 생성하는 두 개의 이미디에스테르 그룹으로 구성됩니다. PVDF 막의 표면에 병원체가 붙잡히면 병원체의 세포를 용해하여 핵산을 추출했습니다. 이 DMP와 PVDF 주사기 필터를 이용한 샘플 전처리 플랫폼은 정교한 기기를 사용하지 않고 손으로 조작할 수 있으며, 30분 이내에 가능합니다. 이런 방법은 지금의 상용하고 있는 추출 제품을 사용하여 추출한 경우와 비교했을 때 이에 필적할 만한 효율을 보여줍니다.

검출을 위한 방법으로 육안으로 바로 확인이 가능한 등온증폭을 이용한 핵산 검출 방법을 개발했습니다. SARS-CoV-2 진단을 위해 등온성 증폭 방법 중 RPA,

HDA, LAMP을 사용했습니다. 3가지의 등온성 증폭 방법 중 LAMP에서 가장 좋은 효율을 보여주었습니다. 여기에 LFA 또는 colorimetric 방법을 사용하면 육안으로 결과를 바로 확인할 수 있습니다. 이러한 방법들을 이용하여 우리는 COVID-19 검출을 위해 23개의 임상 검체에서 이 방법의 가능성을 입증했습니다.

다음으로, 포인트 돌연변이의 검출은 분자 표적화, 맞춤형 약물 전달, 치료 진행 및 종양의 약물 저항성 모니터링에 큰 이점을 가지고 있습니다. 기존 돌연변이 검출 기술은 비용이 많이 들고 복잡하며 대립 유전자에 특화되어 있거나 한 번에 다중 탐지를 허용하지 않습니다. 그래서, 우리는 새로운 기법으로 hot spot-specific probe (HSSP)를 이용하여 대장암(CRC) 환자의 조직 샘플에서 KRAS 돌연변이를 검출하는 기법을 개발했습니다. 추가적인 단계 없이 높은 감도와 빠른 속도, 간단한 분석 방법으로 돌연변이를 검출할 수 있습니다.

본 연구에서 제안된 샘플 준비 기법은 소량 또는 많은 양의 임상 샘플과 함께 사용할 수 있는 간단하고, 신뢰할 수 있는 민감도를 가지는 저렴한 플랫폼을 제공하므로 다양한 감염성 질병에 대한 엄청난 유용성을 가지고 있습니다. 또한, 육안으로 확인이 가능 한 등온성 증폭법을 이용한 검출 기술 및 HSSP를 사용하는 검출 기법은 이러한 팬데믹 시대에 의료진의 부담을 줄이기 위한 사전 선별 플랫폼으로 가정 및 클리닉에서 COVID-19 같은 감염성 질병 혹은 암과 같은 질병에 대한 간단하고 편리하며 효율적이며 저렴한 진단 분석을 제공합니다. 함께, 제안된 기술(샘플 준비 및 검출기법)의 통합은 임상 응용 분야에서 기존 방법보다 빠르고 저렴한 진단 분석을 제공할 수 있습니다.

Keywords: Molecular diagnostics, Sample preparation, Point-of-care test, Mutation detection;